



University of
Stavanger

Faculty of Science and Technology

MASTER'S THESIS

Study program/ Specialization:

Engineering Structures and Materials – Civil
engineering structures

Spring semester, 2022
Open

Authors: Mehari Tsadik Gebremeskel and
Arve Tuvera Cruz

Faculty supervisor:

Associate Professor Mudiyan Nirosha Damayanthi Adasooriya

Thesis title:

Fatigue life assessment of a steel bridge based on measured corrosion wastage and actual
traffic loading

Credits (ECTS): 30

Keywords:

Fatigue assessment

Corrosion

Steel road bridge

Fatigue load model

Alternative load model

Pages: ...86...

+ Appendix: ...8...

Stavanger, 15. August 2022

Master's Thesis

Fatigue life assessment of a steel bridge based on measured corrosion wastage and actual traffic loading

By

Mehari Tsadik Gebremeskel and Arve Tuvera Cruz



**Faculty of Science and Technology
Department of Mechanical and Structural Engineering and
Materials science, University of Stavanger, Norway**

Stavanger, August 2022

© 2022 Mehari Tsadik Gebremeskel and
Arve Tuvera Cruz

Master thesis
Fatigue life assessment of a steel bridge
based on measured corrosion wastage and actual traffic loading

Distributed by :
Department of Mechanical and
Structural Engineering and Materials science
University of Stavanger (UIS), Norway.
<https://www.uis.no/nb>

Submission date : 15th August, 2022
Faculty Supervisor : Associate Professor Mudiyan Nirosha Damayanthi Adasooriya (UIS)

This document was prepared using L^AT_EX

Abstract

Most steel bridge failures and collapses demonstrate that environmental influences substantially impact the structural integrity of steel bridges. Fatigue and corrosion have been recognized as the primary aging processes for steel bridges, especially in marine environments. Acknowledged gaps in research due to the absence of detailed guidelines for evaluating structural integrity in relation to fatigue and corrosion are problematic. Additionally, the absence of general S-N curves for structures of steel prone to corrosive environments, alongside the lack of research on both fatigue and corrosion increasing the vulnerability and failure of steel classes used in bridges, makes the estimation of the fatigue life of steel bridges uncertain. Estimating the remaining service life accurately is crucial to using the available infrastructure efficiently.

This thesis determines a more accurate fatigue life for steel road bridges based on measured corrosion wastage and actual traffic loads. Corrosion fatigue, one of the main factors in reducing the fatigue life of a steel bridge, is explored at the same time. A conventional approach (Miner's rule) and two current proposed methods are used alongside different scenarios of actual traffic loads to calculate the fatigue life of a specific steel bridge (Storåna I bridge in Norway). A database gathered from the bridge's visual and technical inspections is used while estimating the fatigue life of the bridge. Moreover, a comparison and discussion of results assembled from the conventional method and the two current proposed methods used alongside different scenarios of actual traffic loads are illustrated within the thesis.

Acknowledgement

This Master's thesis is our last project for the Master of Science degree in structures and materials from the University of Stavanger, Faculty of Science and Technology, Norway. The study was conducted during the spring semester of 2022.

We want to convey our deepest gratitude to Associate Professor Nirosha D. Adasooriya, our supervisor at the University of Stavanger, for her assistance throughout the thesis. The advice and help with the research and her direction on the structural analysis and calculations of the case studies have been beneficial and greatly appreciated.

Furthermore, our thanks and heartiest appreciation go to Professor Sudath C. Siriwardane from the University of Stavanger. He has been an enormous help throughout the thesis by giving us challenging concepts and models. It has been a delight to work under his supervision. We appreciate Professor Sudath's constant guidance, time, and motivation alongside Associate Professor Nirosha D. Adasooriya.

Last but not least, we would like to thank our families and friends for their unwavering support and encouragement throughout our work on the thesis.

Thank you all!

Contents

Abstract	i
Acknowledgement	ii
List of Figures	ix
List of Tables	xi
Abbreviations	xiii
Symbols	xiii
1 Introduction	1
1.1 Background	1
1.2 Research problem	1
1.3 Research objectives	3
1.3.1 General objective	3
1.3.2 Specific objective	3
1.4 Significance	3
1.5 Scope	4
1.6 Limitations	4
1.7 Outline of the thesis	4
2 Literature review and theory	6
2.1 Background	6

2.1.1	History of fatigue	6
2.1.2	Impact of fatigue	7
2.1.3	Factors of fatigue process	7
2.2	The fundamentals of fatigue	9
2.2.1	Crack initiation	9
2.2.2	Crack propagation	10
2.2.3	Final failure	10
2.3	Fatigue stress	10
2.3.1	Nominal stress analysis	11
2.3.2	S-N curve	11
2.4	Limit states for steel bridges	12
2.4.1	Fatigue limit state	12
2.4.2	Main parameters influencing fatigue life	13
2.5	Miner's fatigue damage theories	14
2.6	Corrosion	15
2.7	Corrosion fatigue	23
2.7.1	The Process of Corrosion Fatigue	23
2.7.2	Prevention of corrosion fatigue	24
2.7.3	Stress corrosion	24
2.7.4	Hydrogen embrittlement	25
3	Methodology	26
3.1	Fatigue assessment approach	26

3.2	Standards of the Eurocode	26
3.2.1	NS-EN 1993-2	27
3.2.2	NS-EN 1991-2	28
3.2.3	NS-EN 1993-1-9 Eurocode 3: Design of steel structures	30
3.3	Models for traffic load	33
3.3.1	Fatigue load models	33
3.3.2	Alternative Fatigue Load Model	35
3.4	Fatigue design	36
3.4.1	Damage Accumulation Method	36
3.4.2	Palmgren-Miner damage accumulation	37
3.4.3	Limitations of the Palmgren-Miner method	38
3.5	Equivalent Stress Method	38
3.6	Definition and applications of influence line on a road bridge	40
3.7	Approach for structural analysis	41
4	Fatigue damage model for improved assessment of remaining life	42
4.1	Proposed fatigue strength of corroded steel	42
4.1.1	Parameters used in the proposed curve	44
4.2	Proposed uniaxial fatigue damage model	45
5	Framework for life assessment	47
5.1	A Conceptual framework for life assessment of steel bridge details	47
5.1.1	Framework-1	47

5.1.2	Framework-2	48
6	Bridge specifics with traffic load models	49
6.1	Bridge description	49
6.1.1	Model of the existing road bridge structure	49
6.1.2	Damage description of the steel bridge	50
6.2	Fatigue load model	52
6.2.1	FLM4	52
6.2.2	Materials properties (Uncorroded and corroded DIP95)	53
6.2.3	Cross section properties of uncorroded members (effective area, second moment area and section modulus)	54
6.2.4	FLM4 for maximum moment at midspan	55
6.3	Fatigue assessment	57
6.4	Alternative Fatigue Load Model	61
6.4.1	Fatigue load analysis results - Maximum moment response	64
6.4.2	Nominal stress results	66
6.5	Nominal stress results based on alternative fatigue vehicle load	67
6.5.1	Fatigue strength for structural steel components (Uncorroded Steel)	67
6.5.2	Fatigue strength for structural steel components	67
6.6	Fatigue damage of corroded steel	68
6.6.1	Using the proposed method for calculating fatigue life	69
6.6.2	Fatigue strength for structural steel components	69
7	Case studies	71

7.1	Case study-1	71
7.2	Case study-2	71
7.3	Case study-3	72
7.4	Case study-4	73
8	Discussion and comparison of the case studies	75
9	Conclusion and future directions	78
9.1	Conclusion	78
9.2	Future directions	79
	References	86
A	Appendix	87

List of Figures

2.1	Corrosion cell	16
2.2	Uniform corrosion [1]	18
2.3	Types of pitting corrosion [2]	19
2.4	Corrosion-fatigue fracture through mild steel sheet, resulting by fluting of the sheet in flue gas condensate [3]	23
3.1	The Eurocode components utilized in bridge design and construction	27
3.2	Concept behind fatigue load models in Eurocode [4]	29
3.3	Detail category of constructional detail in the Eurocode [4]	30
3.4	Fatigue strength curves for direct stress ranges	31
3.5	Fatigue assessment of bridge structures by Eurocodes	34
3.6	Load function of a vehicle	40
4.1	Schematic representation of fatigue strength curve of uncorroded and corroded details categories	43
5.1	Conceptual framework-1 for estimating fatigue life of corroded structural members	47
5.2	Diagrammatic depiction of the proposed damage transfer concept [5]	48
6.1	Storåna I Bridge	49
6.2	Longitudinal section of bridge	50
6.3	Non Composite Rolled Steel Beams	50
6.4	Girder with corrosion	51
6.5	Corroded DIP 95 cross section at midspan of exterior girder with 4mm uniform corrosion at top and bottom flange bottom surface.	52
6.6	Five standard lorries for fatigue load based on Eurocode	53

6.7	Uncorroded DIP95	54
6.8	FLM4 for maximum moment at midspan	56
6.9	Notional lane and remaining area	57
6.10	Transverse axle position	58
6.11	Fatigue assesement	60
6.12	Fatigue load analysis results - Maximum moment response	65
6.13	Design S-N curve for detail category 160	67
6.14	Schematic representation of fatigue strength curve of uncorroded and corroded details categories	69
A.1	87
A.2	88
A.3	89
A.4	89
A.5	90
A.6	90
A.7	91
A.8	91
A.9	92
A.10	92
A.11	93
A.12	93
A.13	94

List of Tables

3.1	Relevant standards for this thesis [4]	27
3.2	Recommended values for partial factors for fatigue strength [4]	32
4.1	Parameters used in the proposed fatigue strength curve of corroded details – Eurocode	44
4.2	Parameters used in the proposed fatigue strength curve of corroded details – DNV code	45
6.1	Girder properties for fatigue verification – Uncorroded Steel [4]	54
6.2	Indicative number of heavy vehicles expected per year and per slow lane	59
6.3	Nominal Stress results based on Alternative Fatigue Vehicle Load	61
6.4	Alternative Fatigue Vehicle Load	62
6.5	Alternative Fatigue Vehicle Load	62
6.6	Probability of occurrence for different scenarios - (1) One lane loaded (2) Both lanes loaded.	63
6.7	Nominal Stress results based on Alternative Fatigue Vehicle Load	66
6.8	Results of damage calculations using the Eurocode-based damage accumulation method and the proposed fatigue damage model.	68
6.9	Results of damage calculations using the Eurocode-based damage accumulation method and the proposed fatigue damage model.	70
7.1	Fatigue life results for case study-1	71
7.2	Fatigue life results for case study-2	72
7.3	Fatigue life results for case study-3	73
7.4	Fatigue life results for case study-4	74
8.1	Comparison of approaches for uncorroded cases-FLM 4	75

8.2	Comparison of approaches for corroded cases-FLM 4	76
8.3	Comparison of approaches for uncorroded cases-Scenarios	76
8.4	Comparison of approaches for corroded cases-Scenarios	77

List of Abbreviations

A	Cross-sectional area
ASCE	The American Society of Civil Engineers
CAFL	Constant Amplitude Fatigue Limit
CSI	Computers and Structures Inc.
D	Total damage
DLDR	Double Linear Damage Rule
EAC	Environment-assisted cracking
FLM 1	Fatigue load model 1
FLM 2	Fatigue load model 2
FLM 3	Fatigue load model 3
FLM 4	Fatigue load model 4
FLM 5	Fatigue load model 5
GDP	Gross domestic product
HCF	High-cycle fatigue
I	Area moment of inertia about the bending axis
LCF	Low-cycle fatigue
M	Design moment
P	Design load
S-N	A stress–life curve (S = amplitude of stress, or nominal stress and N = number of failure cycles)
Y	Distance from the neutral axis

List of Symbols

$\Delta\sigma$	Stress range
$\Delta\sigma_C$	Reference value of fatigue strength
$\Delta\sigma_D$	Stress range at constant amplitude fatigue limit
$\Delta\sigma_L$	Stress range at variable amplitude fatigue limit
σ_{max}	maximum stress value
σ_{min}	minimum stress value
N_R	Number of cycles a stress range can withstand
γ_{Mf}	Partial factor for fatigue strength
γ_{Ff}	Fatigue factor
$\sigma_{D,cor}$	stress range at intersecting points of two slopes of fatigue curve of the details, exposed to corrosive environments
$N_{f,LCF}$	is the number of cycles to fatigue failure of the details when stress range transits from the high cycle fatigue to the low cycle fatigue region
$\Delta\sigma_{cor}$	the fatigue strength range of structural details in corrosive environments
n_i	Number of cycles required for a constant level of stress
N_i	Number of total cycles

1 Introduction

1.1 Background

Steel bridges are subjected to multiple recurring traffic loads that may be substantially under their structural resistance limit. A single application of load would not result in an anomalous consequence, but structural damage accumulated continually over a period of time results in localized and cumulative failure processes known as fatigue. Moreover, when these structures are exposed to aggressive environmental conditions, the steel bridges risk the time-dependent loss of protective coating, a material loss due to corrosion. Thus, if the steel is present in a corrosive environment and exposed to alternating cyclic stresses, then the steel is subjected to corrosion fatigue. Sandviknes et al. [6] note that the damage from corrosion fatigue is almost always more significant than the damage from fatigue and corrosion.

Material loss due to corrosion causes surface roughness, irregularities, corrosion pits, and minimization in the cross-sectional characteristics of the members. The deterioration process caused by environmentally assisted cracking will result in the degradation of material strengths, affecting a bridge's integrity. A reduction in remaining fatigue life is expected in these bridges due to stiffness and structural behavior changes [7].

Although fatigue is one of the most critical forms of damage potentially occurring in steel structures and principal failure modes, fatigue is still less understood regarding the cause of formation and failure mechanism. As the service life of existing steel bridges is also limited by fatigue, significant attention should be given to the aging issues of bridges for which replacements are not economical. Consequently, searching out innovative methods and creating improved technologies for capturing the fatigue phenomena and undertaking a reliable assessment of the fatigue damage state of steel bridges is vital. Doing so serves as a vital component in a nation's transportation infrastructure [5, 7].

1.2 Research problem

Over an extended period, the strength and serviceability modes of failure have been well investigated in the professional engineering communities. Various research studies have uncovered and simulated these effects. The main flaw in structure design or evaluation of recommendations is that time alongside fatigue strength curves for materials dependent on corrosive media materials have not been discussed. The guidelines are specified by codes and standards and are only provided in some countries. The environment-assisted fatigue damages

are pretty significant, and the presence of reliable methodologies and theories is essential.

What is still challenging and unsolved is the accurate prediction of the fatigue damage and the remaining fatigue life of the steel bridge. Numerous investigations have been conducted into fatigue damage evaluation and life prediction of steel bridges using deterministic or probabilistic methods. Siviero et al. [8] and Siwowski et al. [9] proposed a simplified assessment procedure for existing bridges. The assessment procedure is mainly based on visual inspections and non-destructive testing. Thus, these techniques cannot identify essential concepts that are supposed to be included in the guidelines, such as internal damage.

Adasooriya et al. [7] declare that detailed provisions and frameworks are not available for assessing structural integrity and propose a generalized formula of the S-N curve for corroded structural details. The proposed curve's applicability and significance are confirmed by performing case studies. Sandviknes et al. [6] applied this proposed S-N curve to estimate the fatigue life of a steel bridge and compared the results with conventional approaches. A conceptual framework for fatigue life assessment of steel bridge details that are corroded and exposed to a corrosive environment is also implied in the study. The assessment was based on the assumed corrosion wastage and standard fatigue load models. Hence, conservative fatigue lives were calculated. As a result, the existing research is inadequate for a more realistic fatigue life for the bridge based on measured corrosion wastage and actual traffic loading.

Aeran et al. [5] point out that existing life assessment suggestions and guidelines are dispersed throughout design and integrity assessment standards and research papers. Furthermore, these requirements are not revised to account for suggested theories and models. Even now, specific inadequacies in the current standards can be addressed. The fatigue damage theory proposed by design and integrity assessment standards might lead to incorrect life estimates during fatigue life estimations based on nominal techniques. Commonly employed damage theories contain flaws that may result in erroneous life projections [5].

On a more critical note, most existing standards fail to consider different approaches in investigating the influence of various traffic loads on the fatigue life of a bridge by comparing uncorroded and corroded structural details. Fluctuations in traffic loads can cause a significant change in material fatigue performance. The influence induced by various factors and wildly different types of actual traffic loads on fatigue strength is a necessary aspect of fatigue research.

1.3 Research objectives

1.3.1 General objective

This thesis aims to spot and assess the potential for improvements in the fatigue assessment procedure. Case studies need to validate the applicability and significance of the proposed generalized formula of the S-N curve for corroded structural details. Sandviknes et al. [6] applied the proposed S-N curve by Adasooriya et al. [7] to estimate the fatigue life of a steel bridge and compared the results with conventional approaches. The assessment was based on the assumed corrosion wastage and standard fatigue load models. Hence, conservative fatigue lives were calculated.

Moreover, another approach designed by Aeran et al. [5] can be used to accurately anticipate the remaining lifespan of existing infrastructures, such as aging oil and gas platforms, aged bridges, and industrial structures. The Eurocode-based residual life calculations may result in a longer lifespan than the structures can support. This demonstrates the significance of employing a precise fatigue damage model. This thesis will calculate a more realistic fatigue life for steel road bridges based on measured corrosion wastage and actual traffic loads.

1.3.2 Specific objective

- Examining a database of a specific road bridge, i.e., Storåna I bridge, acquired from Statens vegvesen (The Norwegian Public Roads Administration).
- Using a conventional method (Miner's rule) and two other approaches (models) proposed by Adasooriya et al. [7] and Aeran et al. [5] to investigate various actual traffic loads.
- Considering two varied traffic loads, i.e., fatigue load model 4 (lorries with different axel specifications) and the alternative traffic load model (a more eclectic collection of vehicles than fatigue load 4).
- Comparing and discussing outcomes gathered from applying the conventional and two proposed models to fatigue load model 4 and alternative traffic loads.

1.4 Significance

This paper might benefit while estimating the fatigue life of a steel bridge when considering various traffic loads alongside different models used to estimate the fatigue life of a bridge.

Additionally, the thesis can be used for research since the methodology can be recreated to investigate the fatigue life of bridges.

1.5 Scope

A database from a specific bridge (Storåna I bridge) is used while applying a conventional method (Eurocode) and two different proposed methods presented by Adasooriya et al. [7] and Aeran et al. [5]. In addition to using these methods, various traffic loads are taken into consideration for the fatigue life assessment of different case studies.

1.6 Limitations

- Only corrosion that has resulted from a marine environment is explored.
- Effects resulting from wind, braking forces, or such are not included in the calculations.
- No fracture mechanics are investigated.
- Only the steel components of the bridge are considered, and the concrete decks and slab reinforcements are ignored.

1.7 Outline of the thesis

Chapter 1: Introduction

This chapter introduces the study by first discussing the background and context, followed by identifying the research objectives. Moreover, the significance, scope, and limitations of the thesis are entailed in this chapter.

Chapter 2: Literature review and theory

This chapter deals with the theoretical part of fatigue theory. A literature review from a history of fatigue, fatigue assessment, and the primary mechanism of fatigue is described. Additionally, the fundamentals of corrosion and corrosion fatigue are included in this chapter.

Chapter 3: Methodology

This chapter comprises the different standards of Eurocode. Furthermore, the various types of actual traffic loads used to calculate the fatigue life of a bridge are discussed. In addition, fatigue designs, equivalent stress methods, and the definition and applications of influence lines on a

road bridge are covered. A brief description of the software utilized throughout the thesis is also provided in this chapter.

Chapter 4: Fatigue damage model for improved assessment of remaining life

This chapter covers the proposed methods for estimating the fatigue life of a steel bridge.

Chapter 5: Framework for life assessment

This chapter discusses the two frameworks utilized to assess the life of existing steel bridge details prone to a measured corrosion wastage.

Chapter 6: Bridge specifics with traffic load models

This chapter includes the specific details of Storåna bridge I in Norway. Furthermore, the various actual traffic loads and the nominal stress results based on alternative traffic loads are entailed in this chapter.

Chapter 7: Case studies

This chapter comprises the various case studies investigated under this thesis.

Chapter 8: Discussion and comparison of the case studies

This chapter compares and discusses the different case studies illustrated in chapter 7.

Chapter 9: Conclusion and future directions

This chapter concludes the thesis by highlighting the main findings and giving future directions.

2 Literature review and theory

2.1 Background

Fatigue is a failure at relatively low-stress levels of structures subjected to fluctuating and cyclic stresses. This type of failure is the single largest cause of failure in metals and is typical for bridges, aircraft, and machine components. Fatigue failure can be catastrophic since the occurrence is sudden. The initiation and propagation of cracks occur due to fatigue, and the fracture surface is typically perpendicular to the direction of applied tensile stress [10].

Siwowski et al. [9] present that among the leading damage causes of existing bridges, failure due to fatigue comes first, accounting for about 38.3 % of total failures. Siwowski et al. [9] declare the results based on a study by Oehme et al. [11], considering different types of steel structures and their causes of failure. Among 128 considered damaged steel structures, 16 were bridges, including railway and road bridges. According to the study, approximately 98 % of the damage occurred between 1955 and 1984. This indicated that most of these steel bridges were riveted. A further study confirmed that fatigue is the primary cause of the failure of steel-riveted bridges.

2.1.1 History of fatigue

In the 19th century, fatigue was considered an uncanny phenomenon in engineering construction materials, as fatigue damage could not be observed, and failure occurred without forewarning. In the 1840s and '50s, the term "fatigue" was coined to characterize failures caused by repetitive loads. In the early 1850s, August Wohler, a German railroad technician, conducted the first significant engineering research on fatigue. As part of the research, Wohler started developing design techniques to prevent fatigue failure. Wohler conducted bending and torsion tests on iron, steel, and other metals under bending, torsion, and axial loads. Wohler further proved that cyclic stresses influenced fatigue and the constant (mean) stresses present simultaneously. As a result, Wohler conducted the first systematized research on fatigue by conducting several laboratory fatigue experiments under cyclic stresses [12].

In the 20th century, an observation regarding repetitive load applications could commence a fatigue process in the engineering material, resulting in the initiation of a microcrack, the propagation of the crack, and the eventual collapse of a structure. Mann et al. [13] assembled literature documents on fatigue drawbacks. These documents covered the period from 1838 to 1990 and included engineering materials, constituents, and structures in four books with an index of themes, years, and authors. Additionally, the years 1837–1994 were investigated by

Schutz et al. [14] by pinpointing fatigue history. Cui et al. [15] also conducted a state-of-the-art review on metal fatigue, focusing on the most recent advancements in methodologies for predicting fatigue life.

2.1.2 Impact of fatigue

Fatigue is amongst the prime causes of fatal mechanical failures of many structures and infrastructures. Such calamitous occurrences happen abruptly and result in substantial human and material losses. Stephens et al. [16] stipulate that while the definite percentage of mechanical failures due to fatigue is nonexistent, numerous studies imply that 50–90 % of all failures are attributable to fatigue. Furthermore, the American Society of Civil Engineers (ASCE) Committee stated that about 80–90 % of malfunctions within metallic designs are linked to fatigue fractures. [17]. After an extensive study report performed in 1983, Reed et al. [18] deduced that numerous mechanical malfunctions are affiliated with fatigue. The report summarized that nearly 61 % of the failures were associated with fatigue, and the three leading causes of fatigue are improper maintenance, fabrication defects, and design deficiencies.

According to the findings, the cost of fatigue-induced fractures can be drastically decreased using appropriate fatigue analysis methodologies and technologies. The complexity of the fatigue mechanism makes the fatigue failure of metal materials, components, and structures less predictable and not entirely understood by designers and engineers.

2.1.3 Factors of fatigue process

The following conditions are vital to the fatigue process [19]:

- Extraneous cyclic loading
- Geometry of the constituent
- Material features
- Impact of the environment
- Endurance limit

Extraneous cyclic loading: In cyclic loading, elements such as stress range $\Delta\sigma$, disparity of force, and the number of cycles are vital. External forces might instigate regular bending or

torsion effects on a structural constituent, along with associated stress conditions in proximity to a potential crack spot. These kinds of scenarios of loading and response are typically known as loading and stress modes. The direction of the stress relative to the crack planes defines the latter term. The primary causes of crack start and propagation are normal stresses initiated by normal and bending modes. In this situation, the usual stresses move the crack planes directly apart [19].

Geometry of the constituent: The majority of structural members feature geometrical or microstructural disjointedness, known as notches. By increasing the object's dimensions or amplifying the notch's local geometry, often the radius, the stresses can be lowered. Enhancing the local geometry of the notch's radius is favored since neither additional weight nor expense is required [19].

Material features: Standard material properties, such as modulus of elasticity, yield strength, and tensile strength, affect the metal's fatigue strength. The fatigue resistance of a material is measured through experimental testing of material samples. The resistance is yielded by applying a constant-amplitude stress range on a material specimen and counting the number of cycles until failure [19].

Impact of the environment: The environment to which a structural component is exposed affects fatigue life. There is a synergy effect between the mechanical-fatigue damage process and the electrochemical corrosion process when welded joints are subjected to recurrent stress in a corrosive environment. Corrosion may cause surface pits that accelerate the crack initiation time. In addition, the corrosion process worsens the situation within a crack close to the crack's front and may significantly accelerate its growth rate. Therefore, in seawater and other corrosive environments, welded structures should always have some corrosion protection. Typically, cathodic protection and protective coatings provide this [19].

At high-stress levels, fatigue life under cathodic protection is approximately 2.5 times shorter than fatigue life in dry air, although cathodic protection is highly adequate at low-stress levels. At small stress ranges, fatigue life is exceptionally close to that in dry air, and it is reasonable to assume a fatigue limit for corrosion prevention. The corrosion process may soften the crack front at low-stress ranges and leave calcareous deposits behind the crack front. The final consequence could result in a crack closure. The curve provides much shorter fatigue lifetimes at all stress levels in an environment devoid of corrosion [19].

Endurance limit: Certain materials have a fatigue or endurance limit, which denotes a stress level at which the material will not fail and can be repeatedly cycled indefinitely. If the imposed stress level is below the material's endurance limit, the structure has an indefinite life. Under benign environmental circumstances, this is typical of steel and titanium. Numerous non-ferrous

metals and alloys, such as aluminum, magnesium, and copper alloys, lack well-defined limits of endurance. In contrast, the S-N reactivity of these materials is gradually decreasing [19].

2.2 The fundamentals of fatigue

Fatigue is the initiation and progressive growth of microscopic damage into a crack or macroscopic damage under repeated stress application. Even when the stress levels are below the material's ultimate strength, cracks can still develop [20, p. 416 - 417]. As long as the structural components are subjected to recurrent cyclic loading or fluctuation loads, a new material failure known as fatigue failure will develop [21, p. 567]. Fatigue failure uses the term catastrophic because failure occurs suddenly within the materials. Moreover, the failure is not readily observable before it happens and is dangerous because of the change in the condition of the material to resist stress.

There are three phases to the fatigue life of material: the initial damage that causes crack initiation; the propagation of the crack or fractures that result in the partial separation of a member's cross-section; and the final fracture of the material.

2.2.1 Crack initiation

In general, fatigue is viewed as a process of crack initiation followed by a period of crack propagation. Fatigue cracks typically begin from the surface of a structural part where fatigue damage originates as microscopic shear fractures on crystallographic slip planes, which is the first stage called crack initiation. Fatigue cracks begun by the recurrent application of loads that separately would be too small to cause failure.

Fatigue crack initiation occurs at a specific point where there is a high concentration of stress, specifically at defects present in the materials, and what happens in the surrounding environment directly impacts the initiation phase of the crack. In most cases, a crack will begin by roughening the surface under cyclic stresses caused by plastic deformation, and this will result in the process of irreversible plastic deformation along with the active slip-bands that cause accumulation of extrusion and intrusion on the surface [19].

2.2.2 Crack propagation

In crack propagation process, the crack spread from the concentrated plastic deformation to a macroscopic size in a direction at right angles to the applied load. The crack grow to be unstable to make the component fracture.

The fracture propagates typically perpendicular to the primary stress (tensile) during the crack development phase. Plastic deformation occurs along the active slip-band, with the maximum shear stress occurring ahead of the crack tip, resulting in the creation of plastic deformation. The crack development and fracture surface are shown by striations or ripples left on the surface due to the crack propagation and fracture surface. The transition between two phases of the fatigue process is typically difficult to describe precisely since it depends on a variety of variables, including the size of the component, the material, and the fracture detection techniques.

Typically, a steel component experiences most of its fatigue life during the crack initiation phase, especially during the high-cycle fatigue (HCF) regime. The majority of the fatigue life in the low-cycle fatigue (LCF) regime (about fewer than 10,000 cycles) is used up by fracture propagation. During crack propagation, localized plastic deformation at the crack tips is formed, despite the applied stress the object is exposed to in each stress cycle is lower than the yield strength of the metal. The applied stress is amplified at the crack tips until the local stress levels exceed the yield strength of the metal, causing a final fatigue failure [19].

2.2.3 Final failure

Finally, the material fails when the fracture has grown to such a size that it is no longer capable of supporting the applied load. A ductile or brittle condition is seen in the eventual failure of materials at the point of failure. When low cycle fatigue failure occurs, the material is considered ductile with significant deformation; when high cycle fatigue failure occurs, the material is considered to be in a brittle state with minimal deformations [19].

2.3 Fatigue stress

When it comes to fatigue damage, the fluctuations in stress are a higher level of significance than the maximum stress; as a result, the amplitude and mean stress are the most important factors to consider when conducting a fatigue assessment. As a result of this development, the stress range has evolved as a critically important design consideration for many applications.

It is taken into mind while calculating the stress range that the difference between the maximum and lowest stress due to cyclic loading is taken into account; the stress range is defined by the Equation below [22]:

$$\Delta\sigma = \sigma_{max} - \sigma_{min} \quad (1)$$

where :

σ_{max} = maximum stress value

σ_{min} = minimum stress value

2.3.1 Nominal stress analysis

The nominal stress is the most straightforward approach to evaluating fatigue life by calculating the bending and axial load of the member. For bending stress occurring under the design loading, the conventional elastic bending equation uses $\sigma = My/I$, where M is the design moment, y is the distance from the neutral axis, and I is the area moment of inertia about the bending axis. For axial stress occurring under the design loading, the equation of stress uses $\sigma = P/A$, where P is the design load, and A is the cross-sectional area. Mean stresses are used to calculate the maximum stress sustained under cyclic loading [22].

2.3.2 S-N curve

Fractures may form in materials and engineering components that have been subjected to enough cyclic stress. This can ultimately lead to the component's failure due to fatigue or other damage. The number of cycles needed to fail the test reduces as the stress level increases. A stress-life curve, also known as an S-N curve, maybe plotted by doing stress tests at different stress levels. Typically, the amplitude of stress, or nominal stress, is plotted versus the number of failure cycles.

There appears to be a distinct stress level below which fatigue failure does not occur under ordinary conditions in mild steel or certain other steels. There is a flattening of the S-N curve that looks to be an approximation approaching the amplitude of stress. Fatigue limits or endurance limits refer to the lower limiting stress amplitudes. Although the S-N curves of many materials do not show a specific endurance limit, they tend to go down as N increases.

The S-N curve is predominantly utilized for high cycle fatigue, which is regarded to exist when the majority of the metal is deformed elastically throughout each cycle. Crack initiation described in 2.2.1 is the primary factor that controls this fatigue regime [23]. When a material undergoes low cycle fatigue, each stress cycle causes it to undergo plastic strain in addition to the elastic strain. Crack propagation described in 2.2.2 is the primary factor that controls this fatigue regime [24]. The gliding transition between these regimes typically corresponds to $N = 10^4$ cycles [25].

2.4 Limit states for steel bridges

Limit state is a condition where a structure or an element of a structure no longer meets performance specifications [26]. The limit state function for fatigue is characterized by two random variables: the number of applied sequences and the number of cycles to failure for a given stress history [27].

The limit states are classified into the four groups listed below:

- Ultimate limit state (ULS)
- Serviceability limit state (SLS)
- Fatigue limit state (FLS)
- Accidental limit state (ALS)

In this thesis, the only limit state explored is FLS.

2.4.1 Fatigue limit state

One of the most critical factors that need consideration while designing bridges is the fatigue limit state. The fatigue limit state function for bridge girders can be expressed as the difference between the section's moment-carrying capacity and the applied load moment [27].

2.4.2 Main parameters influencing fatigue life

In structural design, the fatigue life of a component is measured by the number of stress cycles it can withstand before failing under repeated cyclic loading.

An important factor in fatigue life is the start or propagation of fatigue cracks under applied stress cycles. According to EN 1993-1-9, the most important parameters are [28]:

- **Stress range**

An influence line approach calculates the maximum stress levels at the points where fatigue evaluation is required. The stress ranges that need to be considered in conjunction with these cycle counts are the maximum point stress ranges on a component for a fatigue vehicle or axle set located anywhere within the structure.

It is taken into mind while calculating the stress range that the difference between the maximum and lowest stress due to cyclic loading is taken into account; the stress range is defined by the Equation 1.

- **Structural detail geometry**

A component's fatigue life and performance under stress and fatigue loads are affected by various factors, including the applied stress range, initial discontinuity introduced during production, and local stress increase arising from the geometry of structural detail.

Discontinuities occur in all fabricated steel constructions due to the steel's production process and the usual fabrication operations of the components. Due to the manufacturing process of the steel and the usual fabrication operations of the components, all manufactured steel structures are subject to discontinuities. The fatigue life of rolled shapes and plate members may be severely reduced by these discontinuities, depending on their size, shape, and composition [29].

- **Material characteristics**

The fatigue life of plain metallic specimens, also known as non-welded specimens, consisting of steel or aluminium alloys, is determined by the composition of the metal and the mechanical qualities and microstructure of the metal. Therefore, since metal has higher tensile strength, it may be possible for it to have a longer fatigue life within the same stress range. This is primarily attributable to a rise in the fracture initiation phase instead of a rise in crack propagation.

- **Environmental influence**

Structural integrity is adversely affected by corrosion. Corrosion fatigue is a form of environmentally assisted cracking that refers to fractures caused by cyclic stress in corrosive environments [30]. The reduction in fatigue strength that corrosion causes has a significant impact on the amount of time the material may remain fatigue-resistant. The fatigue life may likely be decreased by more than 60 percent in circumstances where there is light corrosion and by more than 70 percent in circumstances where there is medium or severe corrosion [31].

2.5 Miner's fatigue damage theories

Fatigue life prediction of onshore and offshore steel structures subjected to changing amplitude loading is a complex problem [32]. Miner's rule is the most straightforward illustration of the damage accumulation model since the model is easy to apply [33]. Miner's rule is a linear damage accumulation theory. The Swede Palmgren proposed the rule in 1924, and Miner refined the rule in 1945. Miner proposed damage law as follows:

$$D = \sum \left(\frac{n_i}{N_i} \right)$$

where, D is the total damage, n_i is the number of cycles required for a constant level of stress and N_i is the number of total cycles can be endured before the i -th constant amplitude loading level fails, given the SN-curve.

Schilling et al. [34] examined the accuracy of the Miner rule for steel bridge members subjected to varying amplitude loadings; root-mean-square had a somewhat better correlation with tests. Nonetheless, the Miner rule is conservative. This discrepancy could result from the Miner rule failing to account for the implications of load sequence. Miner's rule may result in inaccurate life estimates since the rule does not adequately account for the damage caused by the loading sequence [35, 36]. Additionally, through the use of tests, Hashin and Rotem [37] indicated that load sequence can drastically impact a specimen's life when subjected to fatigue variable amplitude loading.

To quantify the fatigue damage caused by variable amplitude loading, specific approaches seek to do so while maintaining the simplicity of the Miner rule and, at the same time, taking into account the effect of load sequence. As a result of the fact that several different empirical fatigue damage theories were developed based on the observation that a fatigue fracture involves both a stage of crack initiation and a stage of crack propagation. Manson and Halford [38, 39] formulated the widely recognized Double Linear Damage Rule (DLDR). As a credible alternative to Miner's rule, the DLDR has been considered. In addition to the stress range

and the cycles, some researchers looked for additional parameters that influence the fatigue damage of steel components. Two examples of such parameters are the mean stress and the stress ratio [40–43].

A significant number of investigations are currently being carried out to find a valid indicator or measure of fatigue damage accumulation under variable-amplitude loading. Aeran et al. [44] provide a precise and straightforward fatigue damage model. The suggested damage model does not involve material testing and is based only on the material's S-N curve or the equivalent detail category. In addition, it does not require a full-range S-N curve. The proposed damage model may be implemented easily by practicing engineers using the partially known S-N curves provided by design standards [44]. Despite its fundamental flaws, the Palmgren-Miner linear damage accumulation model is still widely used in design due to its simplicity.

2.6 Corrosion

Corrosion is the destructive attack and degradation of material (both metallic and non-metallic) in contact with its environment. Degradation results from electrochemical reduction reactions between the material and the setting for a majority of metals and metallic alloys [45]. Corrosion can affect a steel bridge's long-term functionality and integrity [46]. To develop corrosion, four conditions must simultaneously be fulfilled. There must be an anode, a cathode, a conduction electrolyte for ionic movement, and an electrical current. If one of the preconditions is absent, no Corrosion will occur [47]. These components are briefly described below.

Anode: The location where oxidation occurs. The metal corrodes by losing electrons and forming discrete ions in the solution.

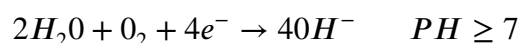
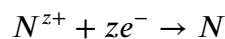


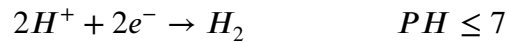
M: a metal

z: the valence of the metal. $z = 1, 2$ or 3 (frequently)

e: electrons

Cathode: the part that usually attracts the electrons created in the anode. The reactions at the cathode consume the electrons. Such reactions can be forming a metal film, reducing oxygen, or hydrogen evolution.





Electrolyte: a solution with enough conductivity to conduct the ions. Water is commonly used as an electrolyte on bridges.

Electrical connection: A connection between the anodic and cathodic sites is needed for corrosion to occur. When the anode and cathode are not made of the same material, a physical connection is required for current flow and corrosion.

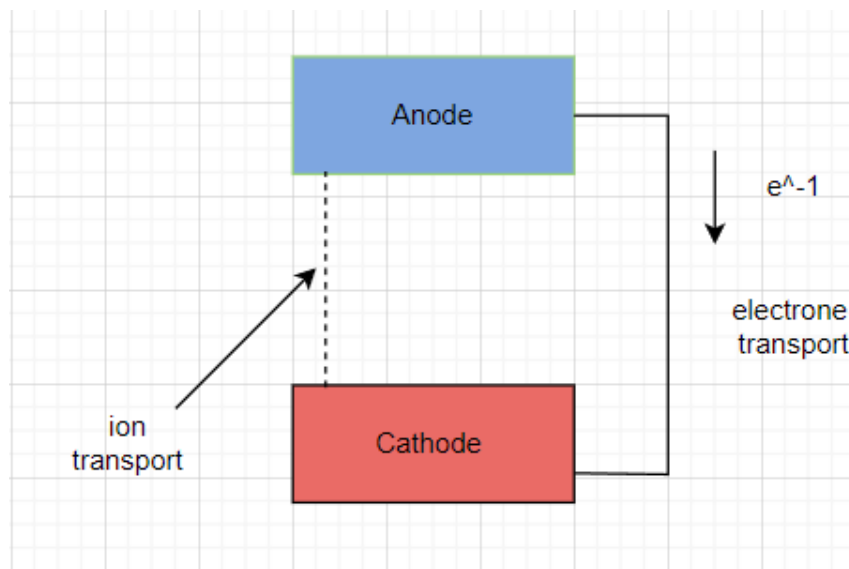


Figure 2.1: Corrosion cell

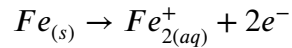
It is always simpler to illustrate corrosion in a primary wet corrosion cell, such as the one depicted in Figure 2.1. Steel corrosion is frequently electrochemical, beginning with the presence of oxygen and water. Carbon dioxide, sodium chloride, and hydrogen sulfide all impede the process.

Corrosion is a series of redox processes that involve the removal of electrons from the metal (oxidation) and their consumption by a reduction reaction, such as oxygen or water reduction. The reduction reaction is frequently referred to as a cathodic reaction, whereas the oxidation reaction is often called an anodic reaction; both reactions are required for corrosion to occur. While the oxidation reaction results in metal loss, the reduction reaction is necessary to utilize the electrons produced by the oxidation reaction to maintain a neutral charge. Otherwise, a considerable negative charge between the metal and the electrolyte would rapidly accumulate, halting the corrosion process.

The description of the corrosion mechanism of iron is as follows:

Iron loses electrons when exposed to moisture (H_2O), forming a positively charged ion in water.

Oxidation reaction: iron undergoes oxidation (losing electrons).

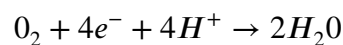


(s): solid

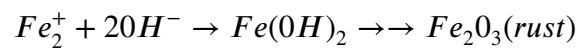
(aq): aqueous

These electrons are then used to decrease the amount of oxygen in the water (H^{+} and OH^{-}).

Reduction reaction: Oxygen is reduced (gaining electrons)



These Fe_2^{+} ions react with the OH^{-} ions in water to form iron hydroxide, which dries in multiple stages to become rust:



Water is required for the redox reaction, explaining why a wet environment accelerates the rusting process. Rusting can occur in dry environments, but it appears much more slowly due to the air's relative lack of humidity [48].

Types of Corrosion

Corrosion occurs in various extensively differing forms. Corrosion can be classified based on one of these three factors mentioned below.

Nature of the corrodent: Corrosion can be observed in wet or dry conditions. Wet corrosion needs liquid or moisture, and dry corrosion usually involves a reaction with high-temperature gases.

Mechanism of corrosion: This requires either electrochemical or direct chemical reactions.

The appearance of the corroded metal: Corrosion is either uniform or localized. The metal corrodes over the entire surface at the same rate when corrosion is uniform and localized, where only small areas are affected [49].

The most important types of corrosion encounters in road bridges may be classified into the following [46]:

1. Uniform corrosion
2. Pitting corrosion
3. Crevice corrosion
4. Galvanic corrosion
5. Corrosion fatigue

1. Uniform corrosion

Uniform corrosion is also known as general corrosion, often occurs in road bridges and is characterized by a corrosive attack that affects the entire exposed surface of a metal or a large fraction of the total area [50]. This type of corrosion is relatively uniform penetration over the entire exposed metal surface, which the human eye can practically see. From a technical standpoint, it is the most accessible type of corrosion to manage because the life of a structural element is accurately estimated based on a comparatively simple immersion test. These tests allow weight loss to monitor and reduce member thickness, thereby the reduction of the effective cross-sectional properties of the members as a function of time can calculate. It is crucial to precisely include the time-dependent effect of general corrosion in the finite element model, using an appropriate corrosion wastage model [2]. Figure 2.2 illustrates a typical uniform corrosion damage.

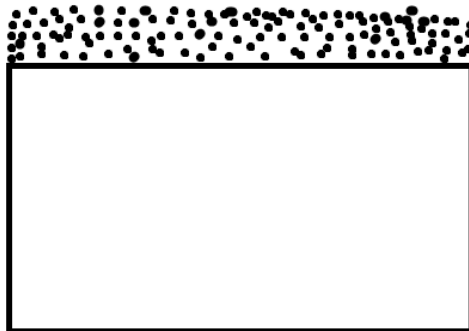


Figure 2.2: Uniform corrosion [1]

2. Pitting corrosion

Pitting is a localized form of corrosion that selectively attacks the surface area of a metal where there is:

- A surface scratch or mechanically induced in an otherwise protective oxide film
- An emerging dislocation or slip step caused by applied or residual tensile stresses

- A compositional heterogeneity such as inclusion, segregate or precipitate [51]

Even though pitting corrosion has no significant effect on the structure's global stiffness, it is dangerous because it can cause local stress concentrations at the structural detail and reduce fatigue. Therefore, it is crucial to consider pitting corrosion while calculating stress concentration factors at the corroded structural element. Figure 2.3 shows a typical Pitting corrosion on steel [2].

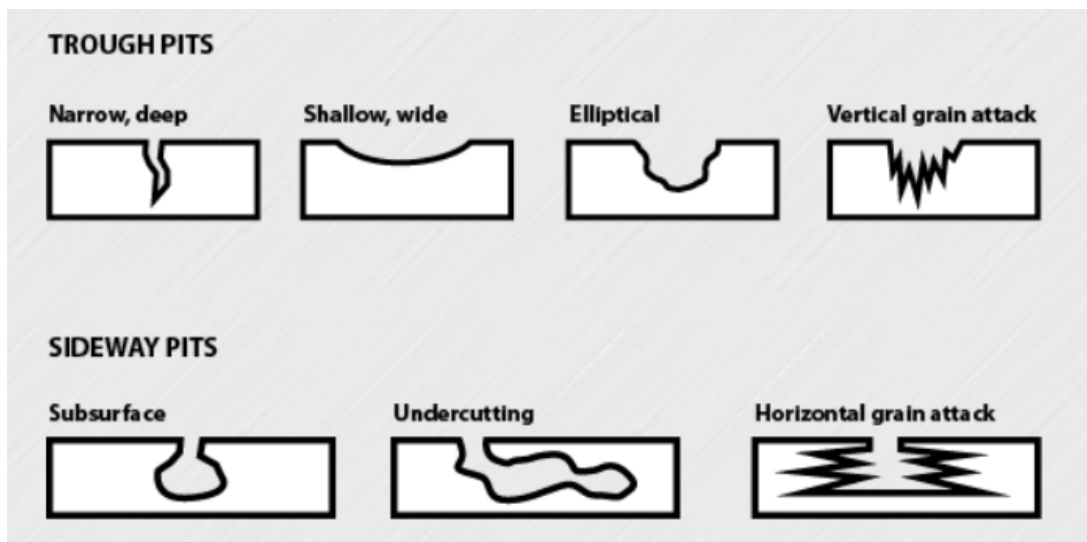


Figure 2.3: Types of pitting corrosion [2]

Crevice corrosion is the most common location-based corrosion on steel bridges. It occurs inside the crevice formed by the contact between two metal surfaces or the surface between a metal and non-metal. A part of the metal that is in contact with unprotected steel elements of a member generates corrosion. Components or elements of the steel bridges prone to Crevice corrosion are, for example, splice plates, gusset plates, and the surface between the bolt/rivet head [52]. In contrast to general corrosion and pitting corrosion, crevice corrosion is often not distinguishable until it becomes critical and can lead to severe problems. An example of connection failure due to crevice corrosion is the Minaus River bridge collapse [52]. Steels that depend on an oxide film for protection, such as weathering steel, are particularly subject to crevice corrosion. High chloride concentrations destroy these films or hydrogen ions that can occur in crevices [53]. The corrosion rate of crevice corrosion is significantly 20 times higher than uniform corrosion [54].

3. Galvanic corrosion

Galvanic corrosion (also called bimetallic) commonly occurs in steel bridges when two different metals are placed in an electrolyte and electrically connected. When a galvanic couple forms, the metal with an initially more negative potential becomes the anode and corrodes. In contrast, the metal with an initially more positive potential becomes the cathode and is protected. Unlike metals must contact with an electrolyte to have galvanic corrosion. The corrosion potential (a

potential variation between the various metals) controls the corrosion rate. Generally, because metals can be sorted into a galvanic series table in terms of their electric potential, galvanic corrosion can occur. The galvanic series lists the electrochemical potentials of selected metals at 25°C in seawater [55].

4. Corrosion fatigue

Corrosion fatigue is the last dominant and dangerous form of corrosion.. It is referred to the mechanical degradation of a material under conditions of simultaneous corrosion and repeated cyclic loading at lower stress levels. Corrosion fatigue can be categorized as a type of environmentally assisted cracking. In section 2.7, the phenomena will be more thoroughly appraised [56].

Factors Affecting Rate and Progress of Corrosion

The environment significantly impacts corrosion and can alter the corrosion rate. Corrosion rate is when a material deteriorates (loss of metal). It is the reduction in thickness that occurs each year and may be computed in general by dividing metal loss by time. Because corrosion rate is one of the most important parameters, it is crucial to investigate how corrosion affects the structural integrity of steel structures and then the corrosion factor . The rate of corrosion is one of the most important elements influencing the service life of a structure. The intensity of the corrosivity is determined by the corrosive environment in which it occurs.

The corrosion rate is frequently prone to change, and it is hard to anticipate when corrosion will occur. Lower PH values, higher concentrations of chloride, sulfate, and carbonate ions, and higher stress levels will all increase the rate of corrosion on steel bridges.

This section will discuss the most significant impacts of corrosion rate on steel bridges.

Effects of corrosion on steel bridges

Corrosion damage is a significant factor in the design of steel bridges. Corrosion's effects on steel bridges can range from minor maintenance issues to catastrophic failures. The Loss of material from the surface, which results in thinner sections, loss of material strength, and deposition of corrosion products (rust) on the surface are the three primary impacts of corrosion on steel structures. Due to material loss, the section properties of a member, such as the second moment of area, area, and the radius of gyration would be diminished, resulting in a decrease in the carrying capacity of the structure [57]. Kulicki et al. [53] recognized four basic categories of corrosion impacts.

1. Loss of section: is the most significant issue to consider. Corrosion's primary effects on steel structures are material loss from the surface, which results in thinner areas, material strength loss,

and the deposition of corrosion products (rust) on the surface. Due to material loss, the section properties of a member, such as the second moment of area, cross-sectional area, the radius of gyration, and so on, would be lowered, reducing the structure's carrying capacity. Bridge members' static, fatigue, fracture, and buckling resistance can be decreased by section loss and the addition of stress raisers. If the metal loss is severe, it may also impact the structure's load distribution characteristics, increasing the load in members next to the deteriorated component.

2. Creation of stress concentration: Corrosion-induced holes and notches cause stress concentrations and can initiate cracks.

3. The introduction of unintentional fixity: When corrosion freezes moving components of the bridge, such as expansion devices or hangers, the structure behaves abnormally. Members may be exposed to unexpectedly high levels of stress.

4. Initiation of unintended movement: According to one study, corrosion products accumulated in restricted areas ("pack rust") can generate up to 10,000 pounds per square inch. This pressure can bend or shift bridge components, resulting in damage [57].

The economic impact of corrosion

Safety, economics, and environmental conservation are the three key concerns that motivate corrosion research. Corrosion-related premature failure of bridges or structures can result in bodily harm or even death. Loss of functioning equipment can have similar catastrophic consequences [58]. Corrosion cost studies have been carried out in several countries, and the results demonstrate that corrosion has a significant influence on the economies of industrialized countries [59]. Numerous industry and infrastructure components, such as bridges, tunnels, and vehicles, are susceptible to corrosion damage. Multiple industries have realized that improper corrosion management can result in significant cost savings over the lifespan of an asset and that improper corrosion management can be highly expensive. The estimated global cost of corrosion is US \$ 2.5 trillion, which is comparable to 3.4% of the global GDP (2013). In 2020, the GDP of Norway was roughly 362.52 billion US dollars. Assuming that 3.4 % of Norway's GDP in 2020 was attributable to corrosion-related damages, this would amount to 12.32 billion dollars [60].

Method for preventing corrosion

Unless rust-prevention measures are adopted, the strength and other attributes of structures constructed of steel will gradually deteriorate over time due to corrosion, which will also shorten the structure's service life. Protecting steel from rust has historically been accomplished using various approaches. The most apparent method is applying a protective coating to steel to protect

its surface from a corrosive environment. Painting, zinc plating, and coating with various oils are examples of this long-practiced technique. Recent protective coatings for the steel include thermal spraying of other metals, organic paints, and lining with rubber or porcelain enamel/plastic film lamination.

Using steel less readily vulnerable to rust is the second method of corrosion protection. Specific components can alter the intrinsic characteristics of steel so that a protective layer forms on its surface during the manufacturing process. Adequate corrosion protection must be balanced with ease of fabrication, dependability, maintenance, and overall cost savings when designing a corrosion protection system. Among these considerations, maintenance is frequently given little consideration during building. Corrosion prevention involves various aspects, the most critical of which are routine maintenance and its economic impact. Even if a corrosion-protection device is an initially successful, chemical or mechanical damage, or even both, eventually degrade its efficiency. Anodes for cathodic protection, organic coatings, and corrosion-resistant steels are all susceptible to corrosion as they age. Corrosion protection requires regular inspections and maintenance, which may be time-consuming and expensive [50].

Environment-assisted cracking

Environment-assisted cracking (EAC) is caused by environmental influences, notably a corrosive environment (EAC). EAC may create damage that is difficult to detect and result in unanticipated failures. In practice norms, there are no detailed requirements or protocols for assessing structural integrity when a structure is subjected to EAC [61].

The formation of EAC is dependent on three factors. These factors describe the mechanism underlying the onset and propagation of cracks in aqueous conditions and demonstrate the significance of developing simplified ways to anticipate EAC [62].

1. Environmental factors such as temperature, pH, pressure, and radiation.
2. Material factors such as tensile strength, grain size, grain boundary segregation, and constitution of phases.
3. Stress factors such as applied or residual stress, stress intensity factor, and tension.

There are three basic types of EAC: corrosion fatigue (CF), stress corrosion cracking (SCC), hydrogen embrittlement (HE), and , which all significantly contribute to the deterioration of metal structures [3].

2.7 Corrosion fatigue

Corrosion fatigue is a product of a corrosive environment and alternating stress [50]. As a combined effect, the two forms of corrosion fatigue are more harmful than any acting alone. When environmental corrosion and vehicle-induced fatigue damage combine, they could cause a catastrophic breakdown that compromises safety and dependability. An essential component of the infrastructure system, bridges are particularly prone to corrosion and fatigue [31]. Regarding road bridge infrastructure, the materials used are subjected to a variety of stresses and corrosion [63]. Particularly extreme situations occur if salt is used to de-ice bridge decks, which melt ice and release brine into the bridge structure. Chemically aggressive conditions are likewise a problem for river bridges [56]. The fall of the Silver Bridge in 1967 was an example of a catastrophic failure resulting from this behavior [64].

2.7.1 The Process of Corrosion Fatigue

Corrosion fatigue is a frequent cause of unanticipated cracking in vibrating metal structures designed for safe operation in the air at stresses lower than the fatigue limit. Cracks caused by corrosion - fatigue are frequently transgranular, as depicted in the figure 2.4. Several cracks can be seen at the metal's surface in the region of the failure-causing crack.



Figure 2.4: Corrosion-fatigue fracture through mild steel sheet, resulting by fluting of the sheet in flue gas condensate [3]

In CF crack initiation and propagation, the stress range and peak stress level are the governing parameters. The commencement of CF cracks may occur in the absence of pits, and the

expansion of CF cracks in carbon steel is due to the post-corrosion reaction [65]. Due to cyclic stresses, grain gliding is visible in some grains. A dislocation's glide is terminated when it reaches a grain boundary [66]. Under reduced load, grain motion retraces the original slip plane. When there are even just a few bumps on the road, it slows traffic and creates a new slip plane. Finally, these disordered bands of material create separation between slip planes at high-stress levels. With decreased activation energy, atoms in a corrosive environment move in a disordered fashion along slip planes. This behavior is possible even at low-stress levels, implying that there is no safe stress threshold beyond which fatigue life is limitless [30, 67].

2.7.2 Prevention of corrosion fatigue

There are multiple methods for decreasing corrosion fatigue. One of the methods to control corrosion fatigue is either a reduction in cyclic stress or corrosion-protection techniques [50]. A protective coating system is the standard practice for shielding steel against corrosion fatigue. Electrodeposited zinc or cadmium act as sacrificial coatings on steel and protect the underlying metal against corrosion in the event of coating flaws. Other repair methods include cathodic protection, inhibitors, and electrodeposits of tin-lead, copper, or silver on steel [3].

2.7.3 Stress corrosion

Stress corrosion cracking is caused by the interaction of tensile tension and a corrosive surrounding. The requisite tensile stresses may be imposed directly or exist as residual stresses. Welding, fabrication, heat treatment, machining, and grinding initiate residual stresses. The inability to anticipate the identification of such minute fissures makes stress corrosion cracking a catastrophic type of corrosion. An unanticipated catastrophic breakdown may result in a low total material loss.

Failures that can arise from stress corrosion cracking depend on the crack size, the intensity of stress, and temperature. This type of failure was exemplified by the 1967 collapse of the Silver Bridge across the Ohio River in the United States, which claimed 40 lives [68]. The bridge structure had eye bars with massive pin connections that could not be inspected. A little crack in one of the eye bars triggered a fracture, which led to the failure of other eye bars owing to overload and the consequent collapse of the entire bridge [50].

2.7.4 Hydrogen embrittlement

Hydrogen intrusion into a component lowers its ductility and load-bearing capacity, leading to cracking and catastrophic brittle failures at stresses much below the yield stresses. Hydrogen embrittlement can cause a component to fail, such as when weldments or hardened steels shatter in the presence of hydrogen. Not all metals are similarly vulnerable to hydrogen embrittlement, and the effect is not permanent. Hydrogen embrittlement may quickly weaken high-strength steels, titanium, and aluminum alloys. Reducing the quantity of in situ hydrogen integrated into the structural part's service life and keeping the steel's residual hydrogen content to an acceptable level are effective ways to prevent hydrogen embrittlement. Despite being discussed in terms of corrosion, hydrogen embrittlement is not technically corrosion [50].

3 Methodology

3.1 Fatigue assessment approach

This chapter provides an exhaustive discussion of the methodology used in bridge fatigue life assessment. The crack growth and the S-N methods are the two methods that can be utilized in order to do a fatigue assessment on the structural components of a bridge. In the crack growth method, the number of cycles required to attain the final crack size is determined based on the beginning crack size, stress range operating on the detail, the average daily number of cycles experienced by the detail, and geometric variables reflecting the stress concentration at the detail. This method determines the number of cycles required to reach the final crack size. The S-N method, which was used in this thesis, calculates the fatigue resistance of a particular detail based on the total number of stress cycles applied to that particular detail. This indicates that the stress range operating on the detail and the number of stress cycles are the most critical elements for a reliable fatigue life estimate [69].

3.2 Standards of the Eurocode

Several standards are connected to the subject of fatigue design. These standards provide regulations and guidance for the design of fatigue in structures. Standards for various loads on structures are specified in Eurocodes throughout Europe. The figure 3.1 presents a listing of the various sections of the Eurocodes relevant to the design of steel bridges and the steel components of composite bridges.

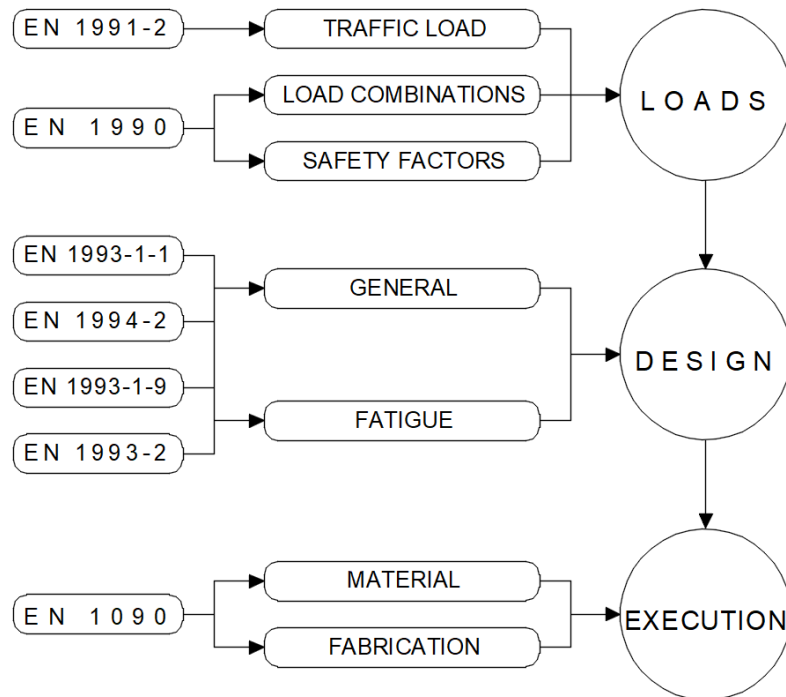


Figure 3.1: The Eurocode components utilized in bridge design and construction [4]

In this thesis, three Eurocodes are studied for fatigue design. These standards are presented in the table below. The reasons behind the selection of these three standards will be described in more detail in sub-sections.

Table 3.1: Relevant standards for this thesis [4]

Standard	Name
NS-EN 1993-2	Eurocode 3: Design of steel structures- part 2: Steel bridges
NS-EN 1991-2	Eurocode 1: Actions on structures- Part 2: Traffic loads on bridges
NS-EN 1993-1-9	Eurocode 3: Design of steel structures- Part 1-9: Fatigue

3.2.1 NS-EN 1993-2

The NS-EN 1993-2 standard provides a general framework for sizing steel bridges and steel components in cooperative bridges. It adds to, modifies, or replaces related requirements in the

various parts of NS-EN 1993-1.

3.2.2 NS-EN 1991-2

The consequences of traffic loads on bridges are typically somewhat complex. In order to address such complicated loading conditions, the "actual" traffic loads must be represented by one or more equivalent load models. Actual loads are required to conduct a fatigue evaluation of a road bridge. In order to accomplish this, the fatigue damage induced by these equivalent load models must be comparable to that caused by the actual traffic load on bridges. NS-EN 1991-2 provides five distinct Fatigue Load Models (FLM) of varying complexity and application scope. On the basis of these concepts, fatigue load models for EN 1991-2 were constructed. In general, the Eurocode fatigue load model derivation approach is shown graphically in figure 3.2 as follows:

- Typical bridges were chosen for modeling bridge responses to traffic flow
- Selection of typical structural components for fatigue analysis and their curves of fatigue resistance
- Performing a simulation of bridge reaction using measured traffic data and the influence line for each examined detail to derive the stress history pertinent to the fatigue design of the detail.
- Utilizing an appropriate cycle counting approach to convert the stress history into a stress histogram with some stress ranges with constant amplitude.
- Applying the damage accumulation rule, also known as the Palmgren-Miner rule, to achieve an equivalent stress range, denoted by the symbol $\Delta\sigma_E$ results in the same damage factor as the stress histogram produced by the traffic simulation.
- Damage-equivalent fatigue load models that yield comparable damage to that caused by $\Delta\sigma_E$ are derived.

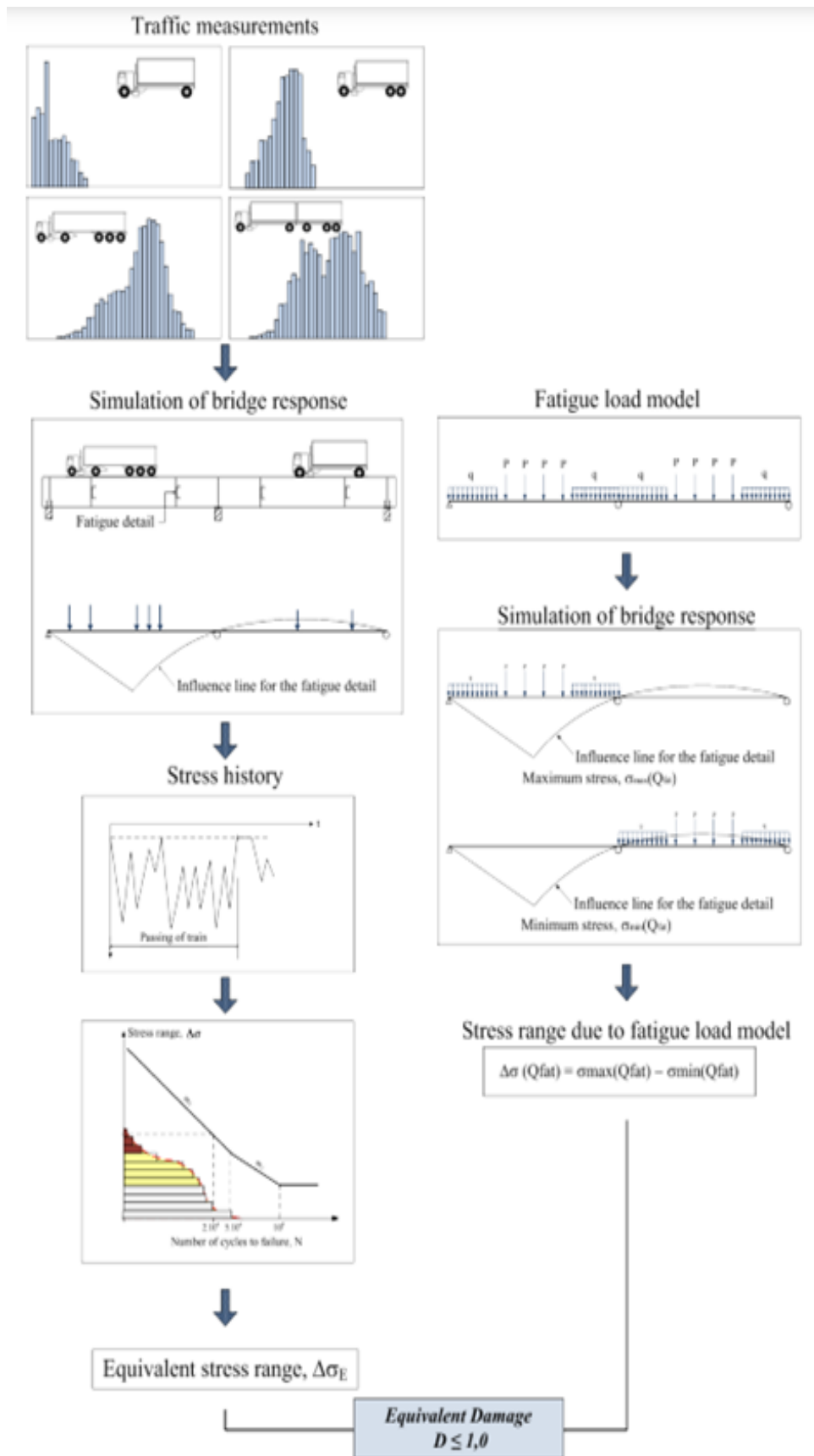


Figure 3.2: Concept behind fatigue load models in Eurocode [4]

3.2.3 NS-EN 1993-1-9 Eurocode 3: Design of steel structures

EN 1993-1-9:2005 provides general requirements and procedures for assessing fatigue in steel structures and their components. This section of the Eurocode applies to all grades of structural steel (including stainless steel) with appropriate corrosion protection and maintenance for the required service life. This indicates that EN 1993-1-9:2005 applies to constructions exposed only to slightly corrosive environments, such as normal atmospheric conditions [4].

The NS-EN 1993-1-9 contains ten detailed categories, numbered 36 to 160. The category number represents the stress range at 2 million cycles with constant amplitude, expressed in megapascals. The matching S-N curve is then generated using test data for specimens of standard geometry subjected to varying amounts of stress. Each number category corresponds to its S-N curve.


Detail category	Constructional detail	Description	Requirements
160	<p>NOTE The fatigue strength curve associated with category 160 is the highest. No detail can reach a better fatigue strength at any number of cycles.</p> 	<p><u>Rolled and extruded products:</u></p> <p>1) Plates and flats; 2) Rolled sections; 3) Seamless hollow sections, either rectangular or circular.</p>	<p><u>Details 1) to 3):</u></p> <p>Sharp edges, surface and rolling flaws to be improved by grinding until removed and smooth transition achieved.</p>

Figure 3.3: Detail category of constructional detail in the Eurocode [4]

Some detail categories are also marked with an asterisk, which indicates that these details are "placed one detail category below their fatigue strength at 2 million cycles." This indicates that their results would not be conservative if they were categorized as if the asterisk was omitted. This pertains to categories 36*, 45*, and 56* of detail. [4]

The S-N curves that are illustrated in this Eurocode are all shifted with one another, and they all adhere to the equation 2 that is stated below:

$$\log N = \log a - m \log \Delta\sigma \quad (2)$$

where

- N: Failure cycles for the specified stress range
- $\log a$: The intercept with the $\log N$ -axis
- m: The negative slope of the S-N curve relates stress range to fatigue life
- $\Delta\sigma$: Stress range

The Eurocode refers to tables 8.1 through 8.10 for the categorization of curve details in order to select an appropriate curve. The designer must select the appropriate detail for the given condition from these tables, followed by the appropriate S-N curve. The curves are displayed in Figure 3.4.

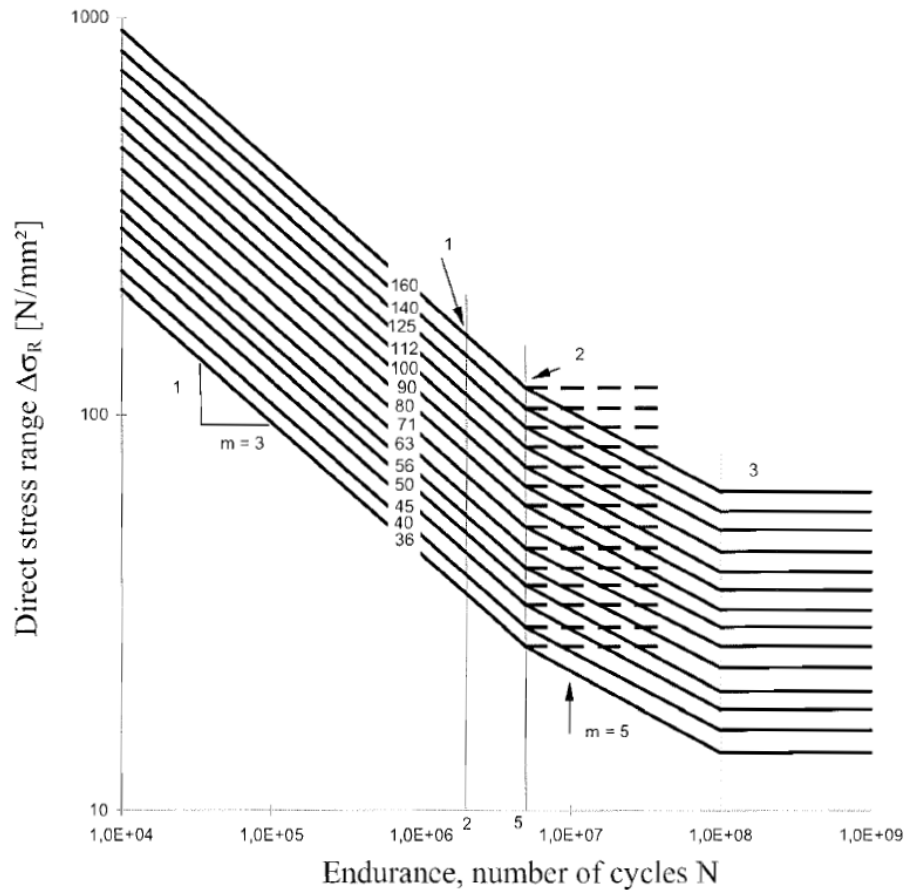


Figure 3.4: Fatigue strength curves for direct stress ranges [4]

The S-N curves are displayed on a logarithmic scale with direct nominal stresses σ_R versus the number of cycles before fatigue damage occurs. The curves for various materials and connections are empirically obtained using several tests for constant stress ranges.

For nominal stress ranges with constant amplitude, the fatigue strength can be calculated as follows:

$$\Delta \sigma_R^m N_R = \Delta \sigma_C^m 2.10^6 \text{ with } m = 3 \text{ for } N \leq 5.10^6 \quad (3)$$

where

- $\Delta \sigma_R$: Stress range
- N_R : The number of cycles a stress range can withstand.
- $\Delta \sigma_C$ is the detail category, the fatigue strength reference value for 2 million cycles.

Direct nominal stresses $\Delta\sigma_R$ are obtained by multiplying stress ranges $\Delta\sigma$ by partial components.

$$\Delta\sigma_R = \gamma_{Mf} * \gamma_{Ff} * \Delta\sigma \quad (4)$$

The recommended partial factor for fatigue strength γ_{Mf} , is stated in EN 1993-1-9 Table NA.3.1 as follows:

Table 3.2: Recommended values for partial factors for fatigue strength [4]

Assessment method	Consequence of failure	
	Low consequence	High consequence
Damage tolerant	1.0	1.15
Safe life	1.35	2.0

This partial factor's value is dependent not only on the safety method, but also on the consequences that might result from the structure failing due to its ultimate collapse. The assessment method (safety method) and consequence of failure from table 3.2 are described as follows:

▷ Safety method

1. **Safe life method** (There are no inspections performed during the service life.)
2. **Damage tolerant method** (periodic inspections are performed during the service life)

▷ Consequences of failure:

1. **Low** for less important members
2. **High** is for important member

When using the safe life method, it is essential to select the appropriate value, as making an error in this selection will significantly impact the life calculations. In this thesis, the safe life method is used.

According to EN 1993-2, the following value is the fatigue factor for fatigue loads:

$$\gamma_{Ff} = 1$$

Equation 3 implies that until $N = 5 \cdot 10^6$, where the constant amplitude fatigue limit $\Delta\sigma_D$ (CAFL) is located, all S-N curves have a negative slope $m = 3$. Constant amplitude loading is a type of cyclic loading that combines constant amplitude and mean load. The CAFL is a stress threshold that indicates that fatigue failure will not occur below this limit under constant amplitude loading. Hence, the CAFL can be calculated as follows:

$$\Delta\sigma_D = \left(\frac{2}{5}\right)^{\frac{1}{3}} \approx 0.737\Delta\sigma_C$$

In figure 3.4, the slope changes from $m = 3$ to $m = 5$ as N increases from $\ast 10^6$ to 10^8 . A horizontal line emerges from the data after $N = 10^8$ cycles. It is presumed that fatigue failure will not occur in low-stress ranges; hence, the component can tolerate an endless number of cycles under stresses lower than this limit. The cut-off limit, often known as the limit for fatigue failure, is denoted by the letter $\Delta\sigma_L$. The cut-off limit can be calculated as follows:

$$\Delta\sigma_L = \left(\frac{5}{10}\right)^{\frac{1}{5}} \approx 0.549\Delta\sigma_D$$

3.3 Models for traffic load

This thesis will analyze two distinct traffic load models:

1. Fatigue load model 4 (FLM4) from NS-EN 1991-2, section 4, subsection 4.6.5.
2. An alternate traffic load model version that attempts to account for all traffic.

Both models are specified under 3.3.1 and 3.3.2.

3.3.1 Fatigue load models

As stated earlier, in section 3.2.2 five fatigue load models are recommended to accurately depict the actual load conditions when building road bridges against fatigue. A precise estimation of fatigue load models for both road and railway bridges involves a proper selection of the geometry of the load model vehicles, their axle loads, axle spacing, and the composition and dynamic effects of the traffic. In Eurocode, traffic load models for bridges have been derived, taking into account all of these elements [4].

The fatigue load models recommended in 3.2.2 for road bridges are based on reference influence surfaces for various types of bridge structures. These structures include simply supported and continuous bridges ranging from 3 to 200 meters. These load models can be split into two major categories based on the required fatigue life. The first group is utilized to confirm infinite fatigue resistance. This category includes FLM 1 and FLM 2. The second category of fatigue load models is intended for analyzing fatigue for a particular fatigue design life using the damage accumulation approach based on the Palmgren-Miner rule or the damage equivalent concept, also referred to as the simplified λ -coefficient method. In this group, FLM 3 is used to calculate the damage equivalent concept, while FLM 4 is used to calculate the cumulative damage concept. The classification of fatigue load models for road bridges is shown in figure 3.5.

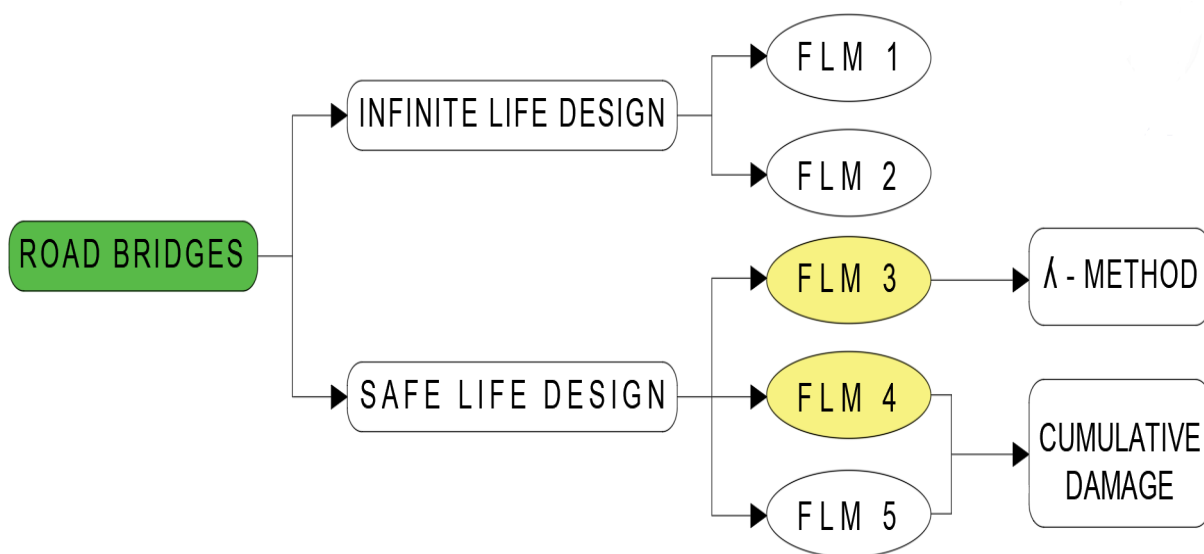


Figure 3.5: Fatigue assessment of bridge structures by Eurocodes

Fatigue load models 1, 2, and 3 aim to estimate the maximum and minimum stresses arising from the various load configurations on the bridge of any of these models. Moreover, models 1 and 2 are primarily used to validate the fatigue resistance of structures for which the so-called cut-off limit described in section 3.2.3. In the case of such constructions, we may determine the direct stress range σ that, regardless of the number of variations in value, does not result in fatigue failure for a specific type of structure or connection. Models 1 and 2 are consequently useful when verifying steel constructions to assess the structure's life due to the onset of fatigue damage. In addition, the model 1 and 2 can be utilized to determine if a load history with a constant stress amplitude has an indefinite fatigue life. Such a method has not been established for concrete structures. Therefore, they lack a specified acceptable stress range whose non-exceedance guarantees a particular fatigue life of the structure regardless of the number of stress cycles [70].

The Fatigue Load Models 3, 4, and 5 are designed to assess a component's fatigue life concerning

fatigue strength curves established in EN1992 to EN1999. The Fatigue Load Model 3 can also be used for the direct verification of designs through the use of simplified techniques. These methods consider the influence of the annual traffic volume and specific bridge dimensions through an adjustment factor that is material-dependent.

The Fatigue Load Model 4 and the Fatigue Load Model 5 are designed to determine the stress range spectra that are the direct result of the movement of vehicles across the bridge. When the simultaneous presence of numerous lorries on the bridge may be overlooked, the Fatigue Load Model 4 provides more accurate results than the Fatigue Load Model 3. This applies to a range of bridges and the traffic that uses them. FLM 5 is the most comprehensive model based on real-world traffic data [71].

Fatigue Load Model 4

The Fatigue Load Model 4 (FLM4) comprises sets of regular lorries that, when combined, provide the same effects as ordinary traffic on European roads. This model replicates traffic that is believed to cause equal fatigue damage to actual traffic. Each conventional lorry is assumed to cross the bridge without any other vehicle. Nevertheless, many national annexes stipulate that 10% of the vehicles on the slow lane must be used concurrently with a vehicle on the adjacent lane [72]. The number of lorries crossing the bridge throughout its design life is determined based on a traffic category and a traffic type, chosen from one of two different tables, namely Table 6.6 and Table 6.2. The tables can be found in the standard NS-EN 1991-2.

According to the NS-EN 1991-2 standard, it is recommended that the category of traffic on the bridge be defined for fatigue calculations based on at least the following criteria:

- The number of slow lanes
- The number N_{obs} of heavy vehicles that is gross vehicle weight greater than 100 kN, seen or approximated, per year and slow lane (i.e., a traffic lane utilized primarily by trucks).

The chosen traffic type and N_{obs} will be presented in the case study in detail. The application of FLM4 to a bridge yields realistic loads in a structure evaluated for fatigue. It is possible to extract a stress spectrum such that a Palmgren-Miner summation can be done in the details where a fatigue crack could develop.

3.3.2 Alternative Fatigue Load Model

Based on fatigue load model 4 from the Eurocode, the alternative traffic load model has been developed to incorporate vehicle classes that depict more realistic traffic. In this proposal, the

traffic parameter known as N_{obs} described in section 3.3.1 for the traffic categories, which refers to the number of vehicles with a maximum gross weight of greater than 100 kN per year per slow lane—has been replaced with yearly average daily traffic. The annual average daily traffic (AADT) is the average daily heavy traffic volume for a particular highway. The projected annual and per-slow-lane vehicle volume is then:

$$N_{alt} = 0.5 \times 365 \times AADT$$

The alternate fatigue load model for road bridges is discussed in length in section 6.3, along with its application.

3.4 Fatigue design

For the fatigue design of bridges, Eurocode permits using two primary methods: the equivalent damage method, often known as the λ -coefficient approach, and the more general cumulative damage method [4]. The simplified λ -method in Eurocode is an adaptation of the general equivalent stress range notion rectified by several λ -factors. In contrast, an alternative to this approach is a direct application of the Palmgren-Miner rule, which may be used for both road and railway bridges [70].

3.4.1 Damage Accumulation Method

Bridge components deteriorate owing to cumulative fatigue damage caused by repetitive vehicle loads, and cracking in the steel girders may begin to occur. This will lead to a reduction in the effective cross-section of the steel girder, which, in turn, will cause an increase in stress. In turn, the increased tension could hasten the onset of corrosion and exacerbate fatigue damage to the bridge. The combined effect of corrosion and overloading will accelerate the bridge's degradation and limit its service life [73]. As fatigue failure results from the cumulative damage produced by each truck passage, an adequate number of stress cycles for fatigue design should consider the influence of each truck passage on the cumulative fatigue damage during the bridge's life cycle [74].

The consequences of traffic loads on bridges are typically somewhat complex. Not only do these loads generate stress ranges with fluctuating amplitudes, but other characteristics that may affect the fatigue performance of bridge details, such as the mean stress values and the sequence of loading cycles, are also entirely stochastic.

It is necessary to characterize the fatigue load effects induced by the "real" variable amplitude loading in terms of comparable, constant amplitude loading in order to be able to tackle such complex loading scenarios. In other words, a complicated loading situation should be represented as one or more equivalent constant amplitude loads in order for the latter to generate equivalent fatigue damage to the actual loading history. Two steps are essential:

- The variable amplitude loading is transformed into a representative constant amplitude loading using a cyclic counting method.
- the new set of representative constant amplitude loading is used to perform the fatigue design or analysis directly by applying the Palmgren-Miner damage accumulation rule or by employing the equivalent stress range concept [70].

3.4.2 Palmgren-Miner damage accumulation

The Palmgren-Miner rule is the best estimate of the fatigue limit and is based on the linear cumulative damage concept [75]. It states that the damage equals the ratio between the number of cycles at a specific amplitude and the number of cycles to failure. At failure, the fatigue life is expended, and the total fatigue damage to the detail is thus 100%, or $D = 1$. If the same detail is now subjected to $n < N$ stress cycles within the same stress range, the accumulated fatigue damage would be calculated as follows:

$$D = \frac{n}{N}$$

giving:

$$D = 1.0 \text{ when } n = N$$

$$D < 1.0 \text{ when } n < N$$

Palmgren initially suggested the above method in 1924 to estimate the life of roller bearers, and Miner subsequently modified it in 1945 to other structural components [76]. The procedure assumes that a component can resist a predetermined number of cycles N_i for a predetermined degree of stress S_i . If the component goes through n_i cycles while subjected to this stress level, then the amount of damage is equal to the fraction n_i/N_i . By adding up all the different k stress levels, cumulative damage can be found [77]. If the stress range distribution function is known, an integral function can be substituted for the summing of the partial damages caused by each stress range level. Failure is characterized by the accumulation of partial damages and happens

when the theoretical value $D_{tot} = 1.0$ is attained . This is represented in the equation below [78].

$$D_{tot} = \frac{n_1}{N_1} + \frac{n_2}{N_2} + \frac{n_3}{N_3} + \dots = \sum_{i=1}^{n_{tot}} \frac{n_i}{N_i} = \int \frac{dn}{N} \leq 1.0 \quad (5)$$

The number of cycles that would induce failure in each stress range σ_i can be estimated directly using Equation 6:

$$N_i = 5.10^6 \left(\frac{\Delta\sigma_D / \gamma_{Mf}}{\lambda_{Ff} \cdot \Delta\sigma_i} \right)^m \quad (6)$$

Where:

m is interpreted as either 3 or 5 according to the stress level [4].

3.4.3 Limitations of the Palmgren-Miner method

Although the Palmgren-Miner rule is a helpful approximation model in many situations, it has the following significant limitations:

- It fails to acknowledge the probabilistic characteristics of fatigue.
- Under certain conditions, low-stress cycles followed by high stress result in more significant damage than the rule predicts. It does not consider the impact of an overload or excessive stress, which can result in compressive residual stress that can inhibit crack formation. Due to compressive residual stress, high stress followed by low stress may cause minor damage. This is represented in the equation below [79].
- It disregards load history, interaction effects, and cumulative damage and has no link to load sequence effects. These are the reasons that led to the development of models of nonlinear damage buildup. These models take load interaction effects into account [80].

3.5 Equivalent Stress Method

The concept of the equivalent stress range underpins the equivalent stress approach. As a result of the Palmgren-Miner rule, the comparable constant stress range correlates to a fatigue life that is identical to the design spectrum if the damage summation is used. After a series of N_F multi-level stress cycles, any stress σ_c equal to or greater than this value will cause the component's failure. Any load with an equal number of cycles in a complex load spectrum will cause damage to the specimen if applied with an equal amount of comparable force [70].

For linear S-N curves with a constant slope of 3, the equivalent stress range for any load spectrum can be expressed as follows in Equation 7:

$$\Delta\sigma_E = \left[\frac{\sum_{i=1}^n n_i \times \Delta\sigma_i^m}{\sum_{i=1}^n n_i} \right]^{\frac{1}{m}} \quad (7)$$

For multilinear (i.e., bi- or tri-linear) S-N curves, the equivalent stress equation is as follows:

$$\Delta\sigma_E = \left(\frac{\sum n_i \Delta\sigma_i^{m_i} + \sum n_j \Delta\sigma_j^{m_i} (\Delta\sigma_j / \Delta\sigma_D)^{m_j - m_i}}{\sum n_i + \sum n_j} \right)^{\frac{1}{m_i}} \quad (8)$$

where:

i is the index of stress ranges with a magnitude greater than $\Delta\sigma_D$ and their respective stress cycles.

j is the index of stress ranges with a magnitude less than $\Delta\sigma_D$ and their associated stress cycles.

m_i represents the slope of the trilinear S-N relationship above the knee point $\Delta\sigma_D$, where $m_i = 3$ stands for structural steel details.

m_j represents the slope of the trilinear S-N relationship below the knee point $\Delta\sigma_D$, where $m_j = 5$ stands for structural steel details.

The transformation from $\Delta\sigma_E$ to $\Delta\sigma_{E,2}$ can be obtained easily from the following equation:

$$\frac{\Delta\sigma_{E,2}^m}{2.10^6} = \frac{\Delta\sigma_E^m}{N} \quad (9)$$

Resulting in:

$$\Delta\sigma_{E,2} = \Delta\sigma_E \left(\frac{N}{2.10^6} \right)^{\frac{1}{m}} \quad (10)$$

The fatigue verification is essentially reduced to a straightforward comparison between the

comparable stress range at 2 million cycles and the fatigue strength of the detail, i.e.

$$\Delta\sigma_{E,2} \leq \Delta\sigma_C \quad (11)$$

All partial factors are eliminated for the sake of simplicity.

Fatigue verification formats using the Palmgren-Miner summation and the similar stress range concept are equivalent in terms of damage and will produce virtually identical results.

3.6 Definition and applications of influence line on a road bridge

The influence line, defined as the reaction curve of a specific point on the bridge under the moving unit concentrated load, includes much information regarding the structure. An influence line represents the variation of a response (reaction, shear, or moment) at a particular point in a member when a concentrated force moves over the structure. The influence line is utilized to establish where the moving load should be put on the structure so that it exerts the maximum effect at the specified spot. After calculating the response caused by this unit load at the region of interest, values are displayed to construct the influence line for the function, where $f(x)$ is the static load function and x_i is position of the axles as demonstrated in Figure 3.6.

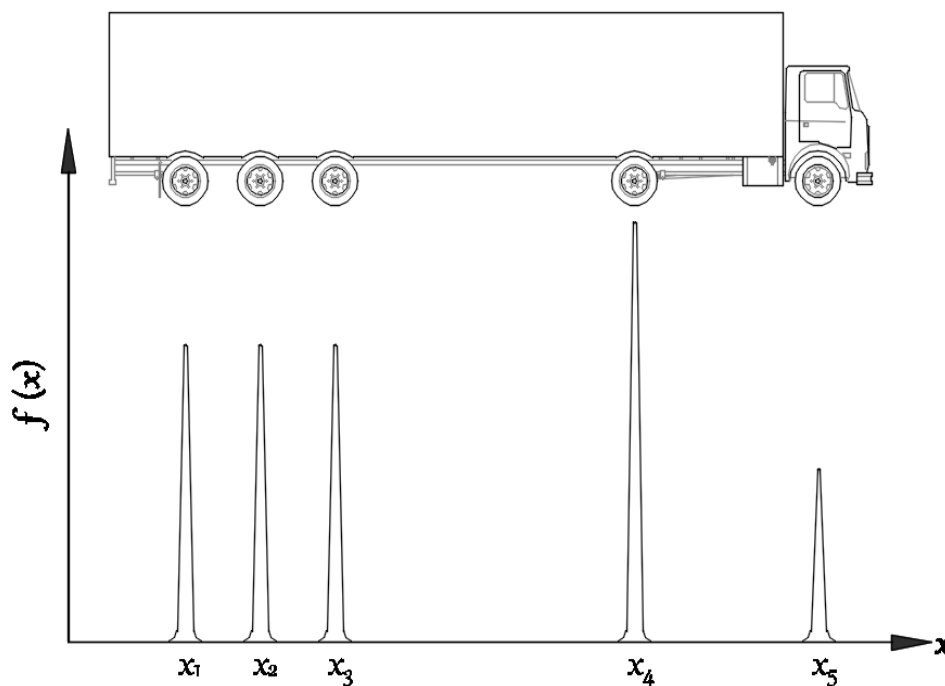


Figure 3.6: Load function of a vehicle

Influence lines have been effectively utilized to update structural models to improve the

prediction of numerical model responses and evaluate engineering structures. In addition, influence lines communicate the structural state and have been used to assess and diagnose structural deterioration [81].

3.7 Approach for structural analysis

A brief description of the software utilized throughout the thesis is provided below.

SAP 2000

The Storåna I bridge is modeled in the FEM-program SAP2000 and AutoCad for the analyses. SAP 2000 is an integrated and powerful tool for structural analysis and design developed by Computers and Structures Inc. (CSI). This software can draw structures ranging from simple 2D to complicated 3D. After drafting and assigning all bridge parameters, moving loads are analyzed. For the sake of simplicity, only one vehicle is allowed to cross the bridge lane at a time [82].

The program can also perform different loading analysis such as: static linear/nonlinear analysis, buckling analysis, influence lines analysis, pdelta analysis, accidental load analysis and vibration analysis. All the capacity checks are based on the given standard and the program compares the acting analysis forces to the sectional capacities. The bridge elements subjected to the maximum stress range were discovered as a consequence of this analysis.

AutoCad

Autocad was chosen as an application program that can interact with programming classes based on a product model since it is the most widely used construction industry program and includes graphical user interface functionality [83]. The geometry of Figure 6.2 was created using AutoCad – 3D program.

4 Fatigue damage model for improved assessment of remaining life

4.1 Proposed fatigue strength of corroded steel

Adasooriya et al. [7] research aims to develop a formula for determining the fatigue strength of structural joints and constructional elements in corrosive media or environments. Based on an experiment conducted by [7], the corrosive environment-dependent parameters were previously determined conservatively. These parameters are derived from corrosion fatigue testing performed on various steels subjected to various conditions. The urban and maritime environments (also known as corrosive environments) and the corresponding constructional detail need to be accounted for in most calculations throughout the fatigue design process (i.e., detail category).

The proposed formula can be easily used with the trilinear or bilinear fatigue curves/S-N curves of defined categories provided in any fatigue design codes of steel structures. However, this is only relevant to the high cycle fatigue (HCF) region. High cycle fatigue is a form of fatigue generated by modest elastic strains subjected to a large number of load cycles prior to failure. Because HCF is driven by elastic deformation, stress is typically a more practical failure criterion parameter than strain. A component's HCF life is often represented as a stress–life curve. The corrosive environment and constructional detail are the key sources of information used by the formula in calculating the parameters. The proposed formula is validated by comparing the experimental results of an extensive number of full-scale experiments performed on corroded structural components.

According to Adasooriya et al. [7] research, the fatigue performance of steel components was significantly affected when they were exposed to environmental conditions. Adasooriya et al. [7] results provided evidence of this phenomenon, which indicates that a modification may be used to describe the design fatigue strength curves of connection categories and detail classes. Thus, this thesis uses Adasooriya et al. [7] model to estimate the fatigue life of members, specifically, uniform corrosion on girders.

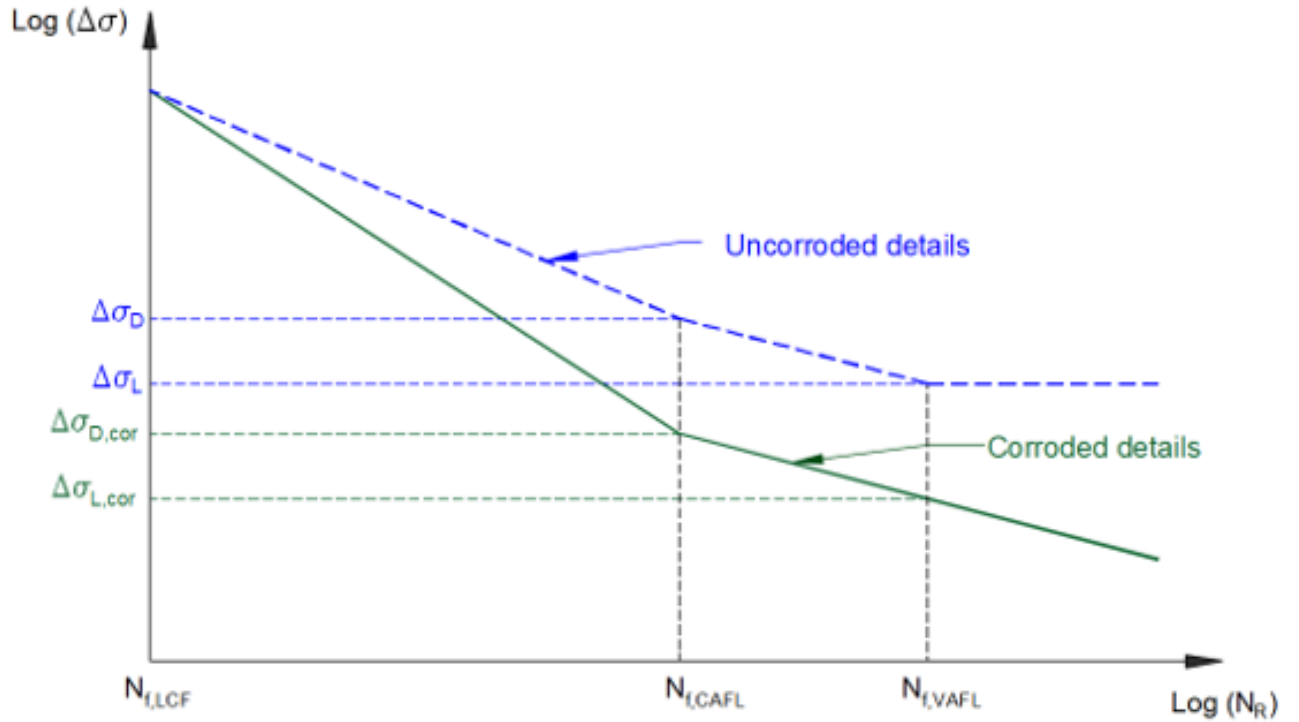


Figure 4.1: Schematic representation of fatigue strength curve of uncorroded and corroded details categories

A proposed formula for calculating fatigue strength has been provided for the corroded detail as follows:

If $\Delta\sigma_{cor} > \Delta\sigma_{D,cor}$

$$\Delta\sigma_{cor} = \Delta\sigma_D \left[N_{f,LCF}^c N_{f,CAFL}^{\frac{1}{m}} \right] N_R^{(-c-\frac{1}{m})} \quad (12)$$

Where $c = \log \left[\frac{\Delta\sigma_D}{\Delta\sigma_{D,cor}} \right] / \log \left[\frac{N_{f,CAFL}}{N_{f,LCF}} \right]$

If $\Delta\sigma_{cor} < \Delta\sigma_{D,cor}$

$$\Delta\sigma_{cor} = \Delta\sigma_{D,cor} \left[N_{f,CAFL}^{-c} \right] N_R^c \quad (13)$$

Where $\Delta\sigma_D$ is the stress range at the fatigue curve slope changing point, which corresponds to

the $N_{f,CAFL}$ cycles, The slope of the fatigue strength curve is $\frac{-1}{m}$. According to the Eurocode, m is equal to 3 when $\Delta\sigma \geq \Delta\sigma_D$, is equal to 5 when $\Delta\sigma_D \geq \Delta\sigma > \Delta\sigma_L$, and it is infinite when $\Delta\sigma \leq \Delta\sigma_L$, $\Delta\sigma_L$ is the fatigue endurance limit of the detail which corresponds to $N_{f,VAFL}$, $\Delta\sigma_{D,cor}$ is the stress range corresponding to $N_{f,CAFL}$ cycles at the intersection of the two corroded fatigue curves, $N_{f,LCF}$ is the number of cycles to fatigue failure of uncorroded details at the intersection point of their HCF and LCF regions.

4.1.1 Parameters used in the proposed curve

To get the values of $\Delta\sigma_D$, $\Delta\sigma_L$, m , $N_{f,LCF}$, $N_{f,CAFL}$ and $N_{f,VAFL}$ for air-tested constructional details, the code provides the fatigue strength/SN curves. $\Delta\sigma_{D,cor}$ and $\Delta\sigma_{L,cor}$ are accountable for the detail's corrosive condition and environmental properties. These properties are often studied using full-scale fatigue experiments, which are expensive in terms of resources and time because of the low loading frequency. Various factors and uncertainties affect the test findings (i.e., experimental fatigue lives). Fracture mechanics theories may be used to estimate $\Delta\sigma_{D,cor}$ and $\Delta\sigma_{L,cor}$ in the case of corrosion pits.

Research shows that carbon steel fractures may develop in any corrosive environment, even when pits are absent. $\Delta\sigma_{D,cor}$ and $\Delta\sigma_{L,cor}$ values for structural steels in freshwater (i.e., similar to an urban environment) and seawater (i.e., similar to a marine environment) may be calculated using the recommended formula for corroded material. Eurocode and DNV fatigue curves may be calculated using the numbers shown below tables.

Table 4.1: Parameters used in the proposed fatigue strength curve of corroded details – Eurocode

Parameter	Construction details in Eurocode			
$N_{f,LCF}$	10 ⁴			
$N_{f,CAFL}$	5 × 10 ⁶			
$N_{f,VAFL}$	10 ⁸			
$\frac{\Delta\sigma_L}{\Delta\sigma_D}$	0.549			
Corrosion parameter	Marine environment		Urban environment	
	Mean value	Conseravtive value	Mean value	Conservative value
$\frac{\Delta\sigma_{D,cor}}{\Delta\sigma_D}$	0.497	0.308	0.641	0.536
$\frac{\Delta\sigma_{L,cor}}{\Delta\sigma_L}$	0.356	0.175	0.518	0.40

Table 4.2: Parameters used in the proposed fatigue strength curve of corroded details – DNV code

Parameter	Construction details in Eurocode			
$N_{f,LCF}$	10 ⁴			
$N_{f,CAFL}$	10 ⁷			
$N_{f,VAFL}$	10 ⁸			
$\frac{\Delta\sigma_L}{\Delta\sigma_D}$	0.631			
Corrosion parameter	Marine environment		Urban environment	
	Mean value	Conseravtive value	Mean value	Conservative value
$\frac{\Delta\sigma_{D,cor}}{\Delta\sigma_D}$	0.46	0.27	0.61	0.50
$\frac{\Delta\sigma_{L,cor}}{\Delta\sigma_L}$	0.356	0.175	0.518	0.40

4.2 Proposed uniaxial fatigue damage model

While several standard codes and research articles guide how to conduct an assessment, these codes have not been updated to reflect the most recent ideas and models. Enhancing the existing guidelines on structural degradation require:

- taking into account the effect of localized corrosion on stress concentration factors,
- selecting proper fatigue strength curves for corroded structural detail categories and
- using more accurate uniaxial fatigue damage models for a better estimation of remaining life are all necessary steps.

An accurate uniaxial fatigue damage model is proposed due to new theories and guidelines. Aeran et al. [44] put forward a uniaxial fatigue damage model. Utilizing nominal and hot-spot techniques and code-supplied S-N curves, the model can be used to predict the remaining life of aging offshore structures accurately. The suggested model requires no additional material parameters and relies on known S-N curves. Practicing engineers can use the S-N curves provided in design codes and standards in various engineering applications. The proposed model is validated using experimental data for several materials' damage curves and fatigue life predictions. This model was chosen for this thesis due to the model's applicability to several engineering fields. In addition, nominal stress analysis is the technique selected alongside code-supplied S-N curves to predict the remaining life validity of aging steel infrastructure in this thesis.

Equation 14 illustrates a simple and effective model for fatigue damage. The material's damage

evolution curve is used to determine the damage for a particular stress level. Once this damage has been transferred to the next stress level, the appropriate number of cycles is determined using the proposed load interaction factor.

$$D_i = 1 - \left[1 - \frac{n_i}{N_i} \right]^{\delta_i} = 1 - \left[1 - \frac{n_{(i+1),eff}}{N_{i+1}} \right]^{\frac{\delta_{i+1}}{\mu_{i+1}}} \quad (14)$$

where:

- D_i is the damage at load level,
- i when exposed to a given stress amplitude (or range) σ_i for n_i cycles,
- $n_{(n+1),eff}$ the effective number of cycles corresponding to σ_{n+1} at level $i+1$, and
- N_i and N_{i+1} are the cycle-to-failure numbers stated in design standards and regulations.

σ_i and μ_i are model parameters that depend only on N and stress levels, as shown in equation 15 and equation 16.

$$\delta_i = \frac{-1.25}{\ln N_i} \quad (15)$$

$$\mu_i = \left(\frac{\sigma_i - 1}{\sigma_i} \right)^2 \quad (16)$$

5 Framework for life assessment

5.1 A Conceptual framework for life assessment of steel bridge details

Essential guidelines based on past studies need to be carried out to identify critical structural members to assess existing road bridges. Contingent on recent research presented in chapter 4, alongside existing guidelines presented in chapter 3, chapter 5 discusses the frameworks utilized to assess the life of existing steel bridge details prone to a measured corrosion wastage. The frameworks are applied to the case studies demonstrated in chapter 7.

5.1.1 Framework-1

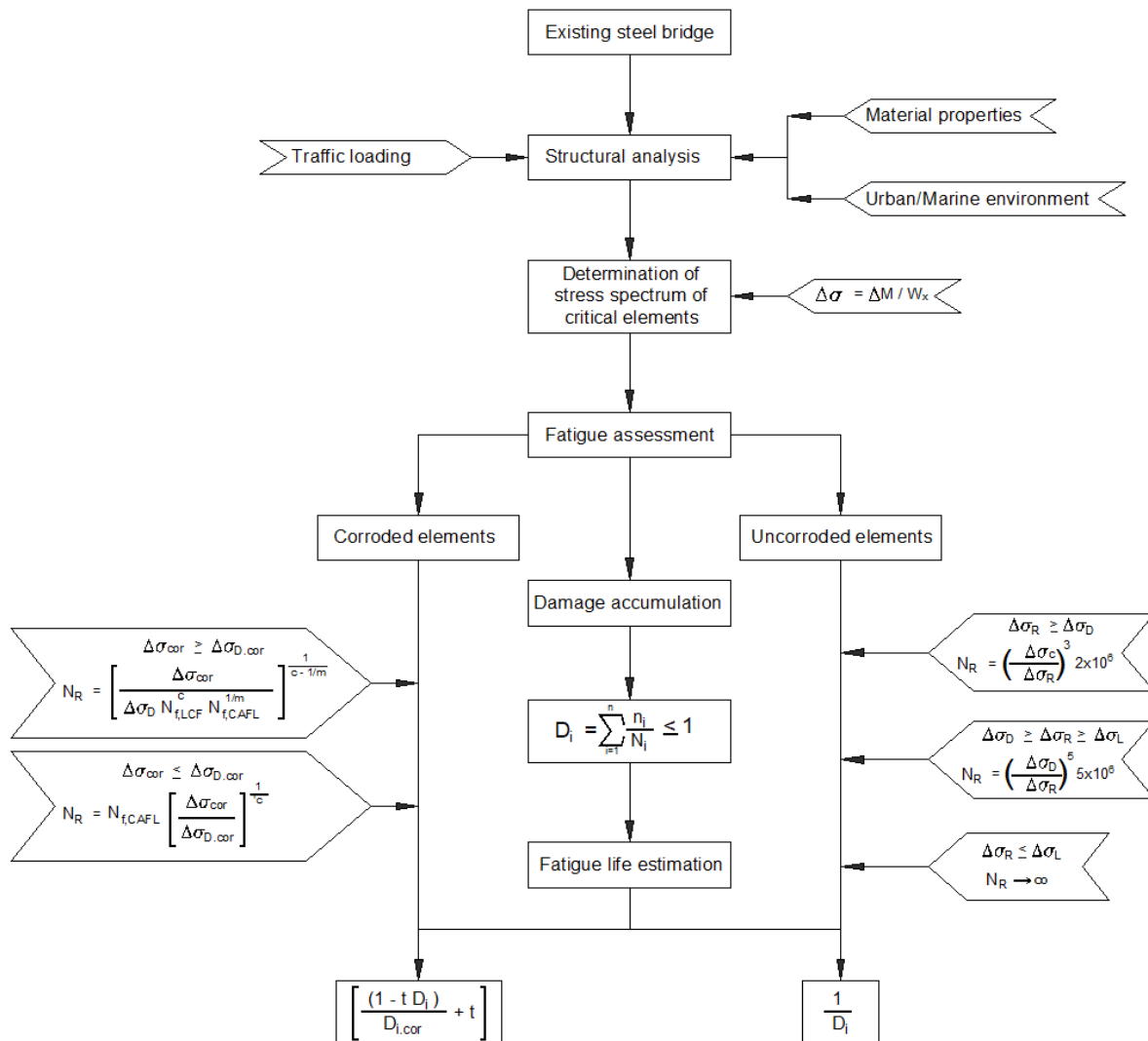


Figure 5.1: Conceptual framework-1 for estimating fatigue life of corroded structural members

Framework-1 is the conceptual framework proposed by Adasooriya et al. [7] for fatigue life estimation. Figure 5.1 is a modified form of the framework designed to be applied to the existing steel bridge. The framework includes determining fatigue life for both corroded and uncorroded materials. The approaches are based on Eurocode's damage accumulation and a newly proposed method for evaluating the service life of members exposed to corrosion and EAC. The structure applies to aging steel bridges in urban or marine environments.

The framework consists of a series of fundamental steps. First, a structural study is conducted to replicate the current state of the bridge and identify the key components. Following this, the stress spectrum of the indicated vital elements must be determined. Then, these are included in the remaining life computation using both the standard and newly proposed methods.

5.1.2 Framework-2

A proven fatigue life estimation method presents a novel notion of damage transfer. This idea relies on fatigue damage progression curves and a hypothesized load interaction factor. This approach to transferring damage is repeated until the fatigue damage D reaches one, signifying failure due to weariness (failure). Using a basic flowchart, as shown in figure 5.2, explains the notion of damage transfer, while the published study provides further information [5].

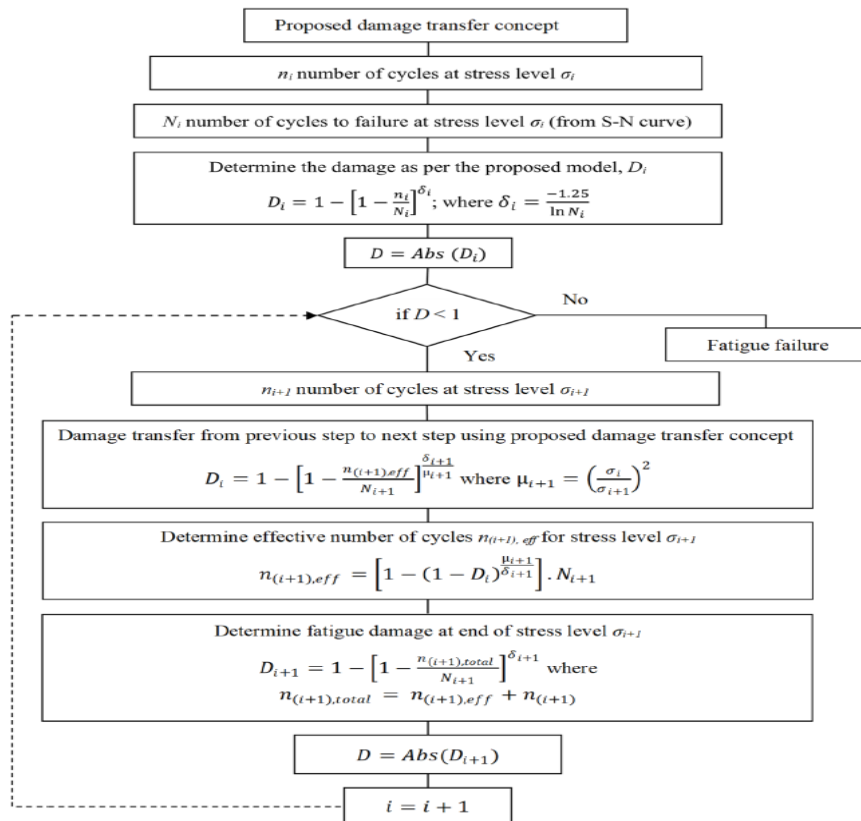


Figure 5.2: Diagrammatic depiction of the proposed damage transfer concept [5]

6 Bridge specifics with traffic load models

6.1 Bridge description

The Storåna I is a road bridge /steel beam bridge and located between Tau (Strand municipality) and Årdal (Hjelmeland municipality) in Norway. The bridge was built in 1937 and partially destroyed by floods. Rebuilt and expanded to what it was today in 1942.



Figure 6.1: Storåna I Bridge

6.1.1 Model of the existing road bridge structure

Existing Storåna I bridge has two simple spans of a non-composite section with an equal length of 19.50m and an end span of concrete tee beam with 12.70m length. It is a two-lane single carriageway where pillars support the superstructure (see Figure 6.2). Layout and sectional drawings are attached in Appendix A.

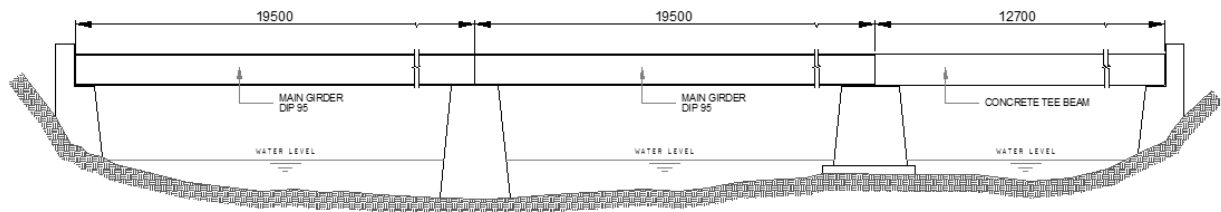


Figure 6.2: Longitudinal section of bridge

The non-composite section comprises a reinforced concrete deck founded on a girder. The girder consists of 3 equally spaced rolled sections DIP 95. The total width of the deck slab is 5.82m, with an average depth of 190mm (Figure 6.3).

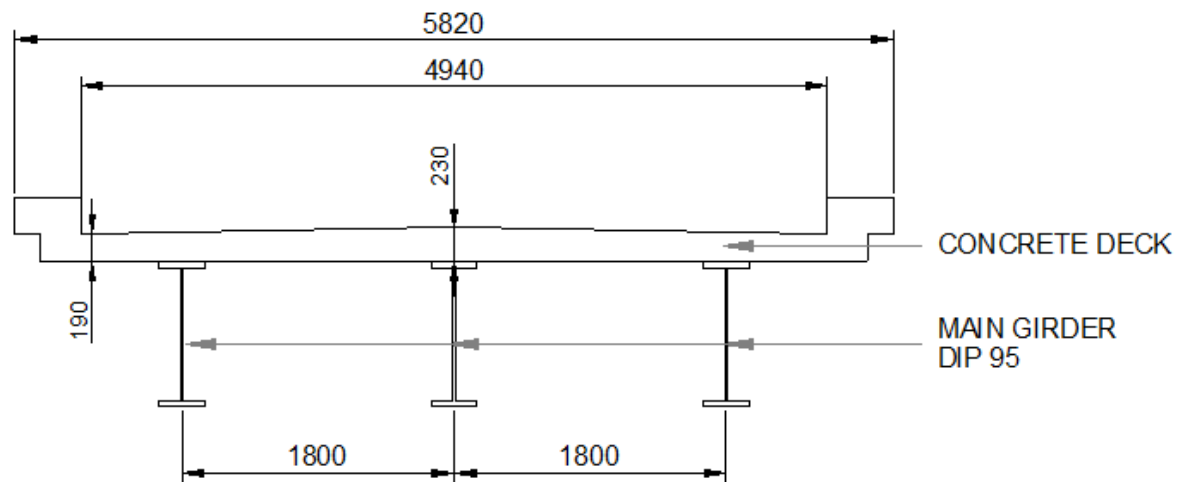


Figure 6.3: Non Composite Rolled Steel Beams

6.1.2 Damage description of the steel bridge

Due to the old bridge structure, increased load cycles, and exposure to a corrosive environment, evidence of coating loss and corrosion is observed in the girder. A maximum of 4mm uniform corrosion is recorded in the midspan of the exterior girder (see Figure 5-3).

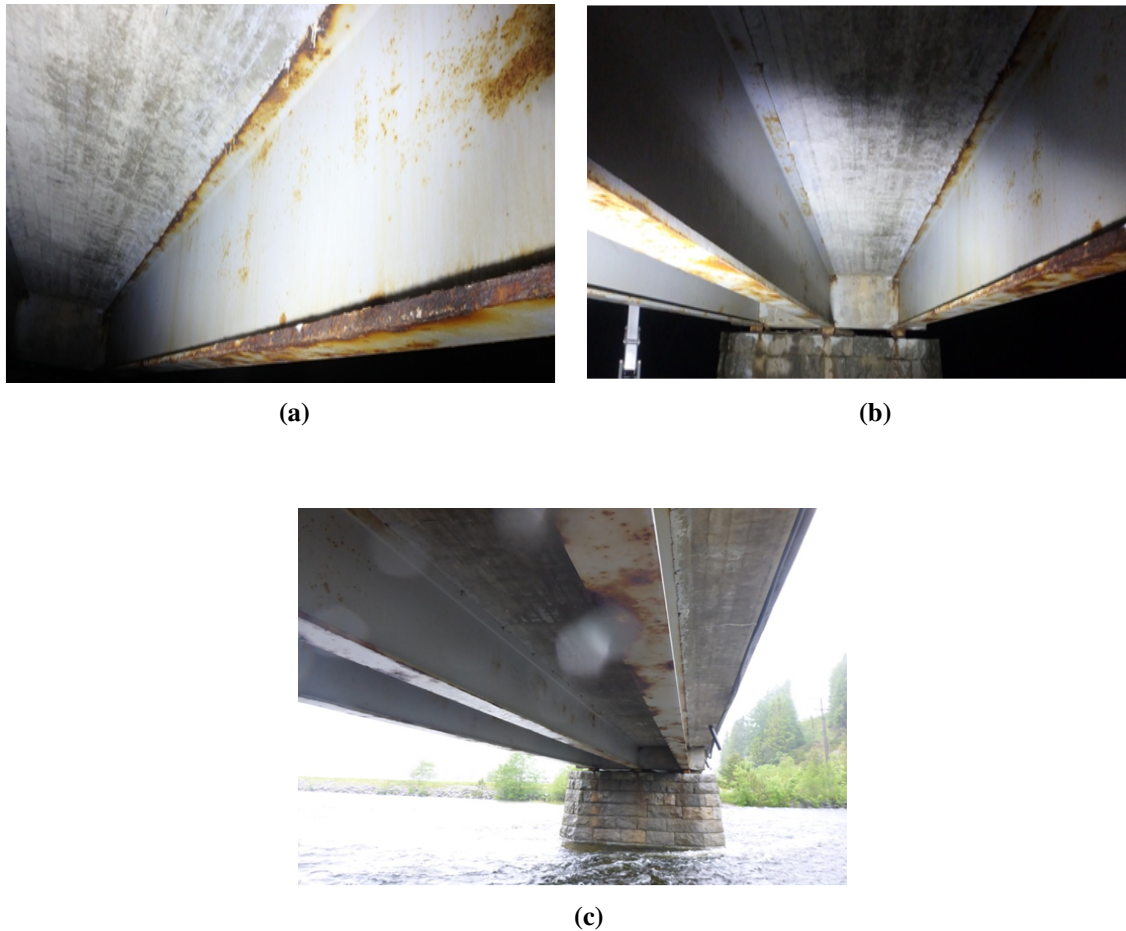


Figure 6.4: Girder with corrosion

It is found that the bottom surface of the top flange is partially corroded, and the bottom and top surface of the bottom flange. This corrosion damage will result in the reduction of geometric properties that govern the structural behavior of the steel (see Figure 6.5). The visual inspection revealed that some areas of the bridge had been exposed to uniform corrosion. There were no visible cracks identified in any portion of the bridge.

Documents such as previous inspection reports and existing drawings record inspection results in the bridge were detailed in the inspection report by Staten vegvesen and will be found in Appendix A.

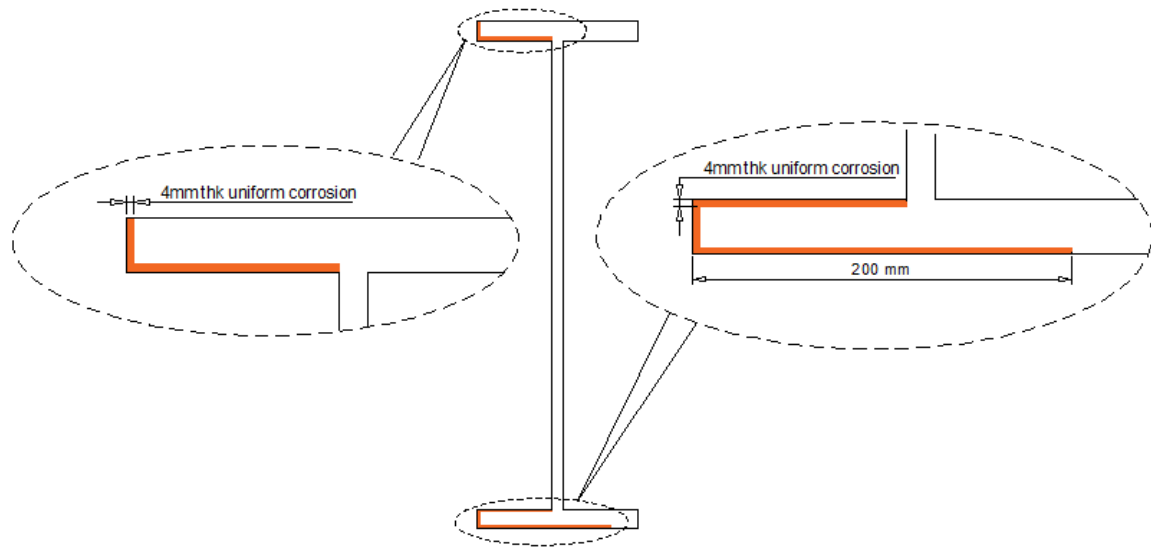


Figure 6.5: Corroded DIP 95 cross section at midspan of exterior girder with 4mm uniform corrosion at top and bottom flange bottom surface.

6.2 Fatigue load model

6.2.1 FLM4

There is no data available for a given bridge concerning the average daily traffic. An approximation from the Eurocode will apply to measure the level of fatigue.

There are five different fatigue load models defined in Eurocode, and Fatigue Load Model 4 (FLM4) is used as recommended for road bridges for calculating the total fatigue damage accumulated through the design service life of the bridge [4].

The set of equivalent lorries and traffic loading is classified as the medium distance used for the simulation of the existing bridge. The axle spacing, equal axle loads, and percentage of heavy traffic according to the road type in each lorry are found in figure 6.6.

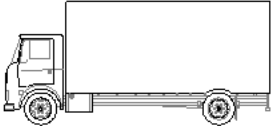
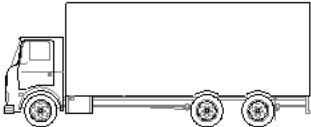
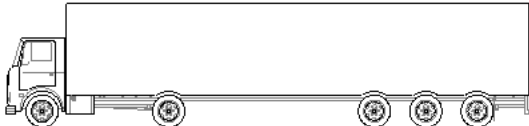
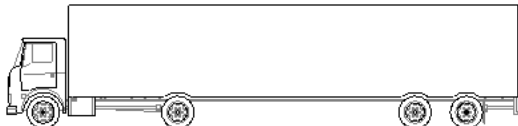
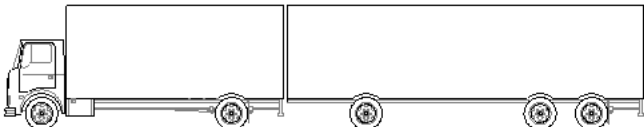
VEHICLE TYPE	Axle spacing (m)	FLM4	
		Equivalent axle loads (kN)	Vehicle % Medium distance
Lorry 1 	4.5	70 130	40%
Lorry 2 	4.2 1.3	70 120 120	10%
Lorry 3 	3.20 5.20 1.30 1.30	70 150 90 90 90	30%
Lorry 4 	3.40 6.00 1.80	70 140 90 90	15%
Lorry 5 	4.8 3.6 4.40 1.30	70 130 90 80 80	5%

Figure 6.6: Five standard lorries for fatigue load based on Eurocode

6.2.2 Materials properties (Uncorroded and corroded DIP95)

Calculation of fatigue assessment is as follows,

- Uncorroded members are in line with the recommendation in Eurocode, which consists of detail category, S-N curves, and Miner's rule is used for remaining fatigue life estimation.
- Corroded members are the application of the newly proposed formula of S-N curves, and Miner's rule is used for remaining fatigue life estimation.

6.2.3 Cross section properties of uncorroded members (effective area, second moment area and section modulus)

Steel beam section : DIP 95

Depth of section (H) = 950 mm

Width of section (B) = 300 mm

Web thickness (t_w) = 19 mm

Flange thickness (t_f) = 36 mm

Structural steel: S275

$f_y = 275$ MPa.

$E = 20$ Gpa.

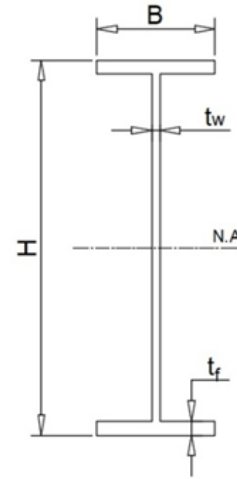


Figure 6.7: Uncorroded DIP95

Table 6.1: Girder properties for fatigue verification – Uncorroded Steel [4]

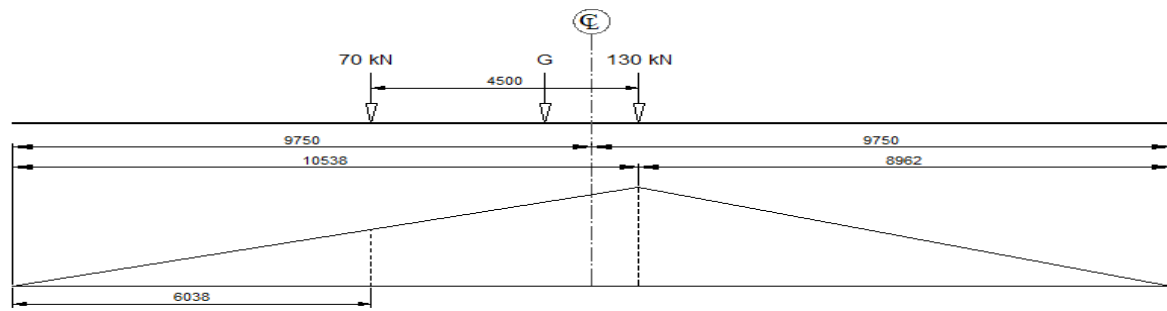
Steel section	Area	I_x [cm^4]	w_x [cm^3]
DIP 95	390.55	572953	12062

6.2.4 FLM4 for maximum moment at midspan

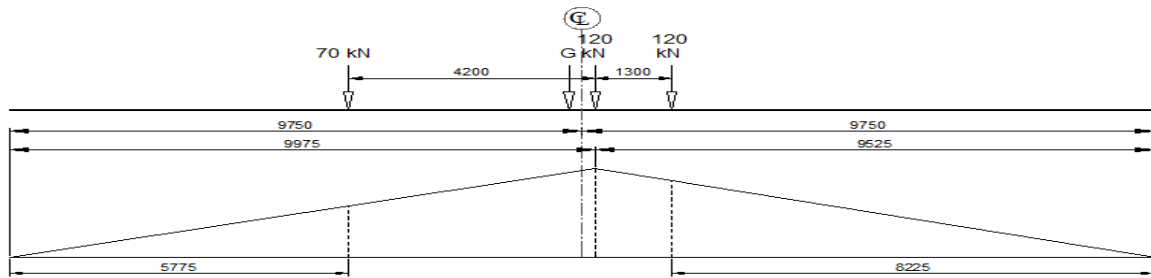
The influence line on a bridge has been presented as a method for studying the bridge's behavior during its service life since it reflects structural behavior under moving vehicle loads [84].

The current bridge has two simple spans of a non-composite section, and due to a typical span of 19.50 meters, a single-span bridge will be modeled. To calculate the moment in girder is by using the influence line to determine the response from the point of interest.

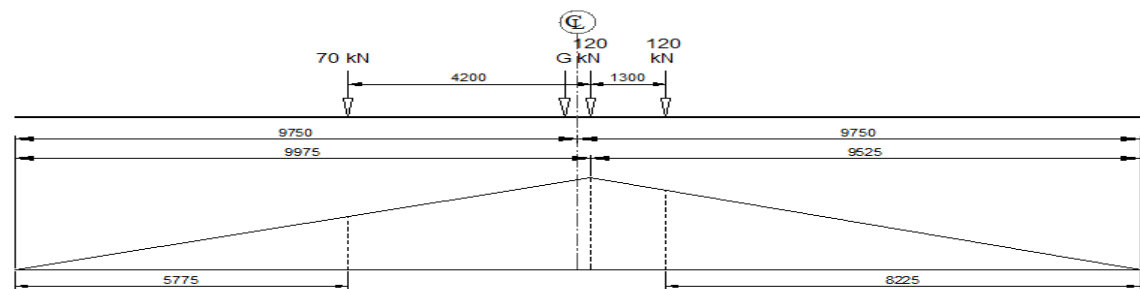
In this thesis, the corrosion is present in the girder's midspan. Therefore, we move the load and put it in the center of the span to determine the response and generate the maximum moment for a single passage of different types of vehicles crossing the bridge as illustrated in figure 6.8.



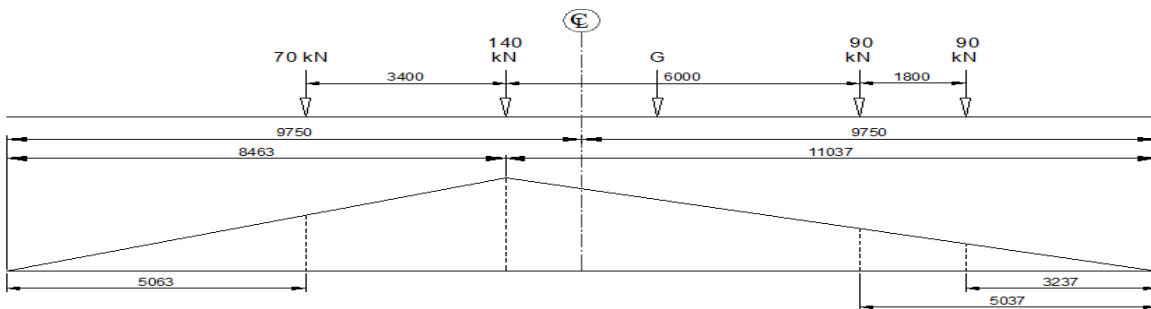
(a)



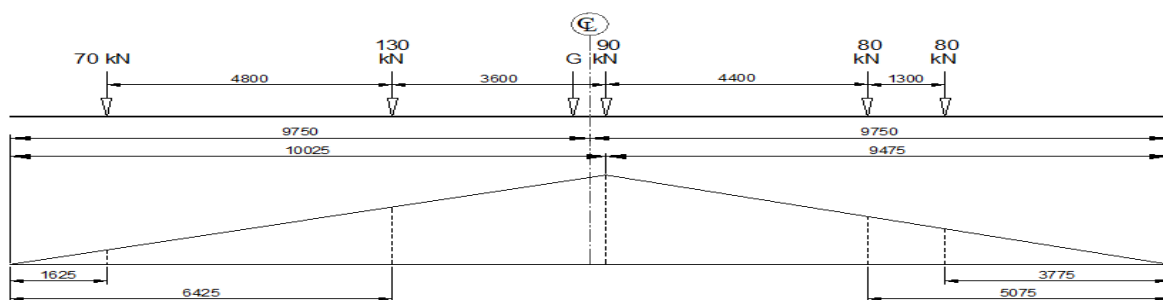
(b)



(c)



(d)



(e)

Figure 6.8: Influence line diagram for maximum moment position in midspan, (a) Lorry 1, (b) Lorry 2, (c) Lorry 3, (d) Lorry 4, (e) Lorry 5

6.3 Fatigue assessment

In defining the stress history from the relevant influence line, simulation of bridge response by fatigue load models is to be considered. Stress history from a single passage is obtained by considering the following steps;

- i. Fatigue assessment for the current bridge classified as a safe life method adopting the recommended value for partial factor for fatigue, $\gamma_{mf} = 1.35$
- ii. Calculate the number of notional lanes and load distribution

The total carriage width of the bridge 4.94m

Notional lane number: $= \eta_1 = 1$

Width of notional lane: $= w_1 = 3\text{m}$

Width of remaining area = 1.94 m

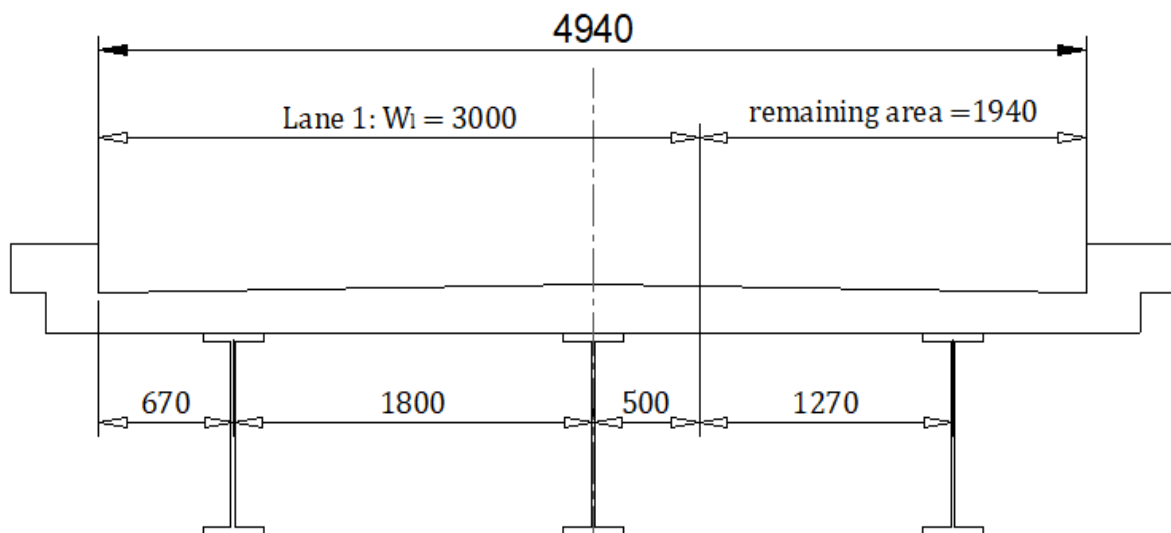


Figure 6.9: Notional lane and remaining area

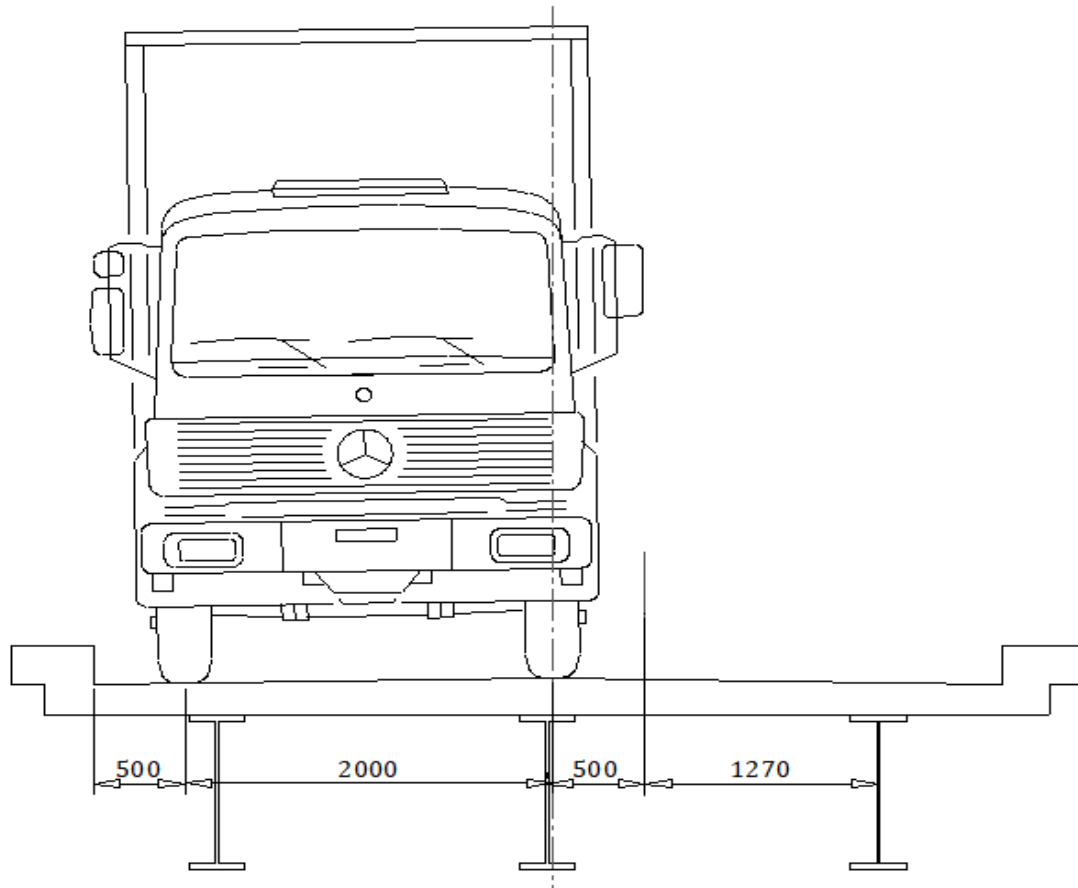


Figure 6.10: Transverse axle position

The complexity of the vehicle's application on the deck slab has led to simplifying assumptions regarding the transverse position of the lorry on the deck slab. For assessing the local effect with notional lanes, Eurocode provides that in transverse position, a single lorry is placed on the span centered in the notional lane.

Therefore, one-lane loading is analyzed using the level rule to determine the load distribution factor to exterior and interior girders.

Load distribution factor for exterior girder = 0.55

Load distribution factor for interior girder = 0.14

iii. Determine the annual heavy vehicles passage to the slow lane.

Table 6.2: Indicative number of heavy vehicles expected per year and per slow lane

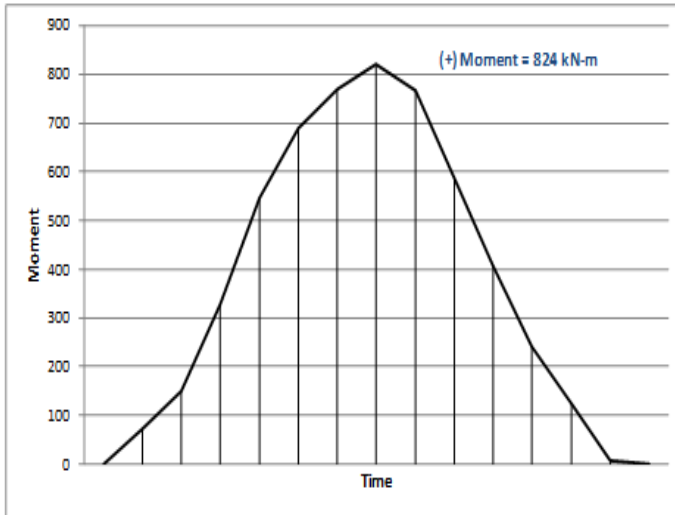
Traffic categories		N_{obs} Per year and per slow lane
1	Roads and motorways with 2 or more lanes per direction with high flow rates of lorries	2.0×10^6
2	Roads and motorways with medium flow rates of lorries	0.5×10^6
3	Main roads with low flow rates of lorries	0.125×10^6
4	Local roads with low flow rates of lorries	0.05×10^6

The total number of lorries crossing the bridge per year is = 125 000. Traffic category 3 – Main roads with low flow rates of lorries.

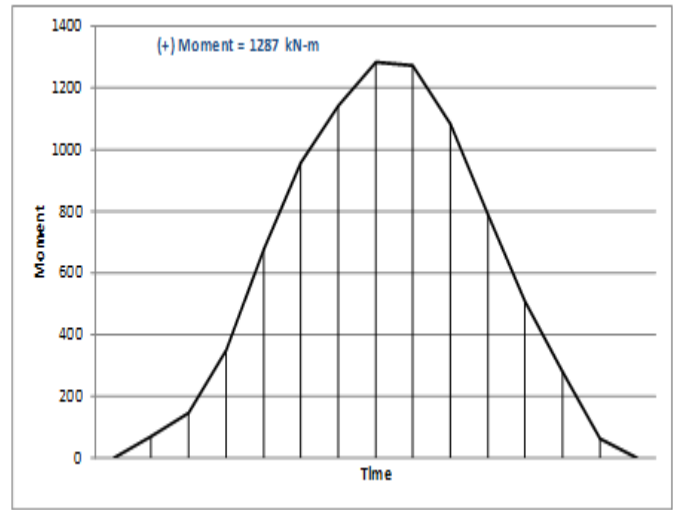
iv. Maximum moment response Since we are evaluating the corroded exterior part of the girder that is in the midspan of the simple span bridge, we have to determine the moment at a location of interest.

The bending moments are established based on the influence line during the passage of each lorry, which will result in a stress history. These moments range during the passage of the lorry is used in place of stress cycle ranges.

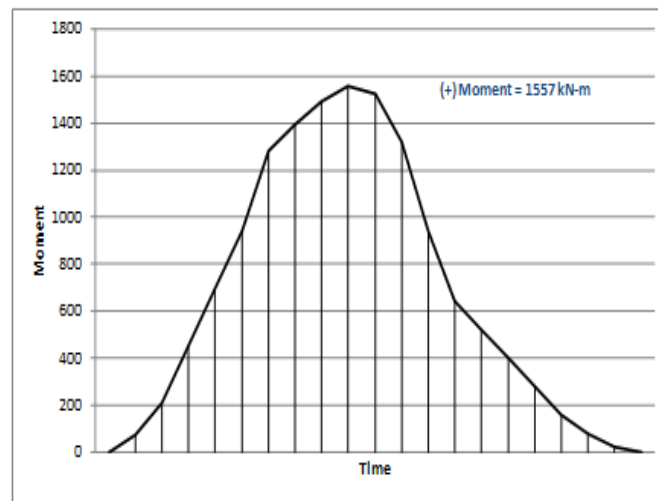
Figure 6.11 show one range of bending moment cycles due to design vehicles crossing the influence line and are used as a reference to compare the corresponding effect for each design vehicle.



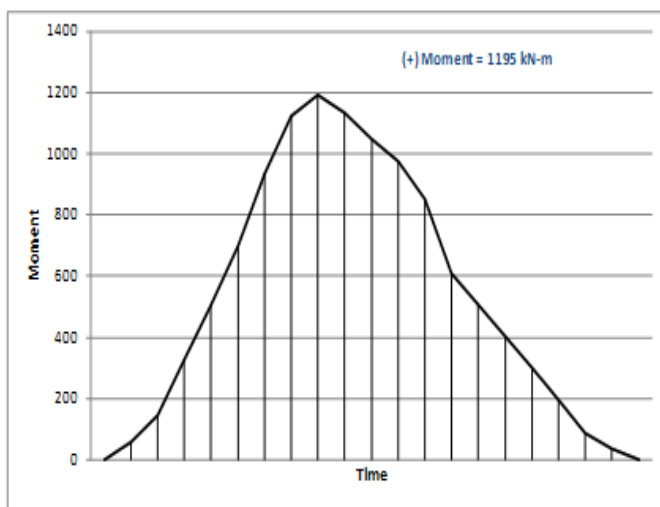
(a)



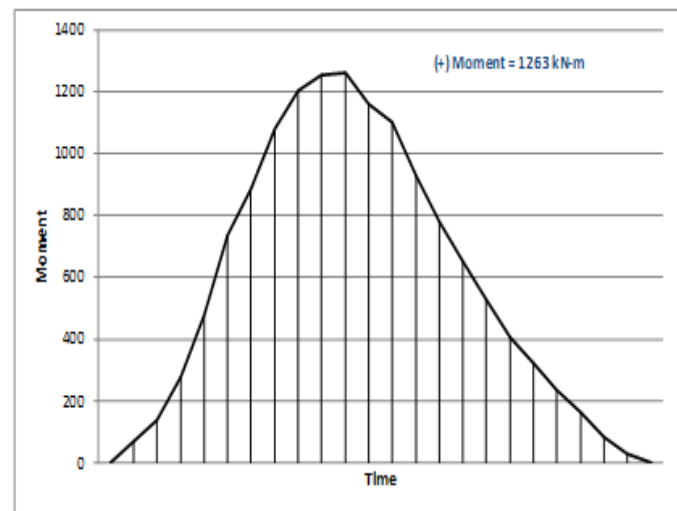
(b)



(c)



(d)



(e)

Figure 6.11: Moment response at midspan considering crossing of five standard lorries in a 19.50m span , (a) Lorry 1, (b) Lorry 2, (c) Lorry 3, (d) Lorry 4, (e) Lorry 5

v. Stress evaluation

For all of the above time histories, the moment is all on the positive side, and it is the maximum moment that dominates and is considered for the fatigue design.

In determining the applied stress range of the exterior girder, the computation of nominal stress is by multiplying the maximum response by the distribution factor divided by the associated section modulus of DIP 95 (corroded/uncorroded state).

Table 6.3: Nominal Stress results based on Alternative Fatigue Vehicle Load

Vehicle type	ΔM_i [KN – m]	Uncorroded		Corroded	
		$\Delta\sigma_i$ [Mpa]	$\Delta\sigma_R$ [Mpa]	$\Delta\sigma_i$ [Mpa]	$\Delta\sigma_R$ [Mpa]
Lorry 1	453.20	37.57	50.72	41.03	55.39
Lorry 2	707.85	58.68	79.22	64.08	86.51
Lorry 3	856.35	71.00	95.84	77.53	104.66
Lorry 4	657.25	54.49	73.56	59.50	80.33
Lorry 5	694.65	57.59	77.75	62.89	84.90

6.4 Alternative Fatigue Load Model

According to Eurocode standards, a more realistic representation of traffic must include in the alternative fatigue load model that derives from FLM4. As a result, an additional six vehicles have been added to accommodate the remaining traffic. The annual average density of traffic (AADT) in the vicinity of the bridges is 2000, which is then used to calculate the number of vehicles anticipated to go across the road bridge.

Table 6.4: Alternative Fatigue Vehicle Load

Vehicle type	Axle spacing (m)	Axle loads (KN)
Kombi	2.5	12 12
Sedan	2.9	16 16
Stationwagon	3.0	19 19
SUV/Minivan	3.1	21 21
Pickup/Van	3.2	29 29
Tracktor/Smaller trucks	3.5	64 64

Probabilities for the six remaining vehicle types have been derived from the distribution of registered cars in Norway, according to Statens Vegvesen (Vegvesen (2015a)).

Table 6.5: Alternative Fatigue Vehicle Load

VEHICLE TYPE	PROBABILITY
Kombi	22%
Sedan	22%
Stationwagon	19%
SUV/Minivan	16.5%
Pickup/Van	12.5%
Tracktor/Smaller trucks	8%

Based on the AADT and the route's location, Vegvesen's (2015b) traffic data estimates that 5% to 20% of all vehicles are heavy vehicles. FLM4 has an 8.56 percent share of heavy vehicles based on the expected AADT and the predicted number of trucks. FLM4 Between 8 and 15% of the five FLM4 cars on the bridge is likely to be accounted for by the AADT. Additional guidelines are provided, consisting of 3 cases that define the percentage of heavy vehicles in FLM4 listed in Table 5-9 to study the impact of increasing or decreasing the number of heavy vehicles on fatigue.

Table 6.6: Probability of occurrence for different scenarios - (1) One lane loaded (2) Both lanes loaded.

Vehicle Type	Alternative Fatigue Load Model		
	Scenario 1	Scenario 2	Scenario 3
Kombi (1)	10.56%	10.0584%	9.35%
Sedan(1)	10.56%	10.0584%	9.35%
Stationwagon (1)	9.12%	8.6868%	8.075%
SUV/Minivan (1)	7.92%	7.5438%	7.0125%
Pickup/Van (1)	6.00%	5.715%	5.3125%
Traktor/Smaller trucks (1)	3.84%	3.6576%	3.40%
Lorry 1 FLM4 (1)	0.80%	1.712%	3.00%
Lorry 2 FLM4 (1)	0.20%	0.428%	0.75%
Lorry 3 FLM4 (1)	0.60%	1.284%	2.25%
Lorry 4 FLM4 (1)	0.10%	0.214%	0.375%
Kombi (2)	10.56%	10.0584%	9.35%
Sedan(2)	10.56%	10.0584%	9.35%
Stationwagon (2)	9.12%	8.6868%	8.075%
SUV/Minivan (2)	7.92%	7.5438%	7.0125%
Pickup/Van (2)	6.00%	5.715%	5.3125%
Traktor/Smaller trucks (2)	3.84%	3.6576%	3.40%
Lorry 1 FLM4 (2)	0.80%	1.712%	3.00%
Lorry 2 FLM4 (2)	0.20%	0.428%	0.75%
Lorry 3 FLM4 (2)	0.60%	1.284%	2.25%
Lorry 4 FLM4 (2)	0.10%	0.214%	0.375%

The percentage of heavy vehicles in FLM4 that should be included in further examination of the bridge's fatigue damage is determined by three cases.

Scenario 1: The alternative traffic load model with 4% heavy vehicles

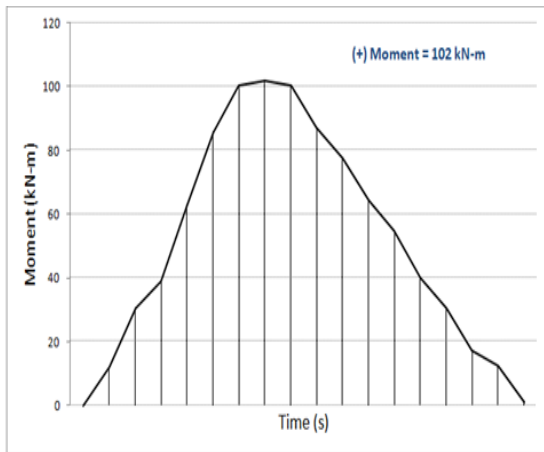
Scenario 2: The alternative traffic load model with 8,56% heavy vehicles

Scenario 3: The alternative traffic load model with 15% heavy vehicles

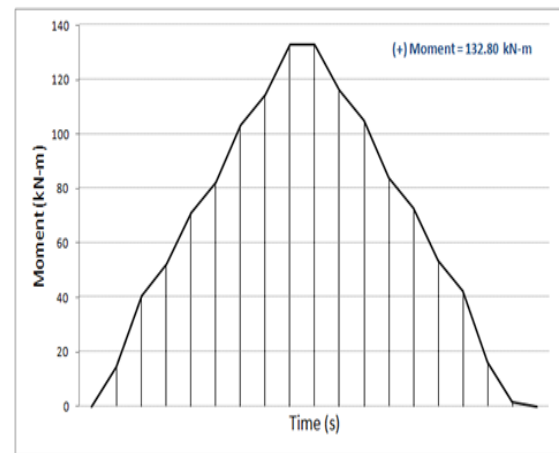
The total number of vehicles crossing the bridge per year is $N_{obs} = 365\ 000$.

6.4.1 Fatigue load analysis results - Maximum moment response

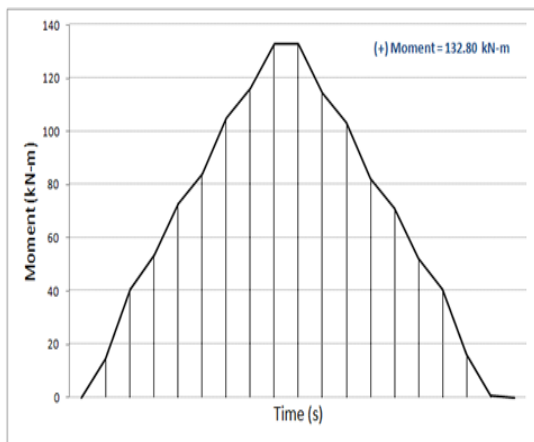
The vehicle fatigue load analysis results are shown in Figure 6.12 using the principles of influence lines. This figure presents the histogram of bending moment responses for an additional six vehicles passing over a 19.50-meter simply supported span about the loading influence of a single traffic lane.



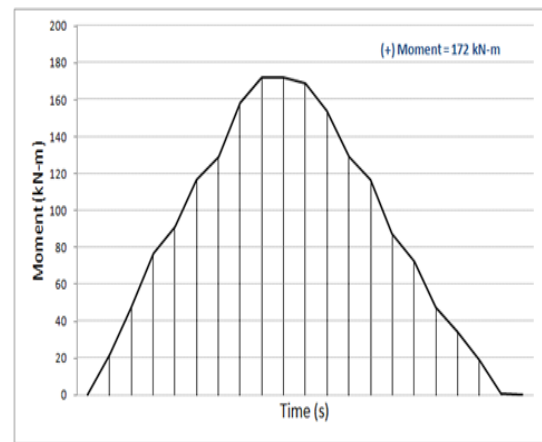
(a)



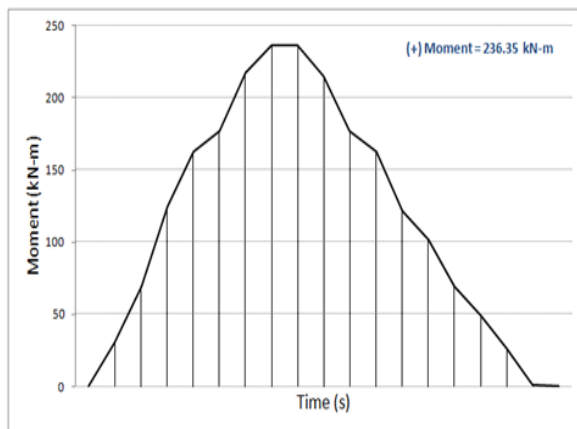
(b)



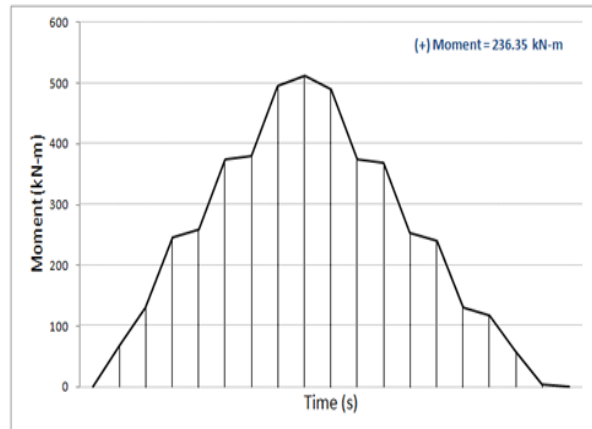
(c)



(d)



(e)



(f)

Figure 6.12: Moment response at midspan considering crossing of six standard vehicles in a 19.50m span , (a) Kombi, (b) Sedan, (c) Stationwagon, (d) SUV/Minivan, (e) Pickup/Tractor, (f) Traktor

6.4.2 Nominal stress results

The calculation for the nominal stress involves multiplying the highest response by the distribution factor and the dynamic amplification factor of 1.30 (NS-EN 1991 -2). The result is then divided by the related section modulus of DIP 95 (corroded/uncorroded condition).

Table 6.7: Nominal Stress results based on Alternative Fatigue Vehicle Load

Vehicle type	ΔM_i [KN – m]	Uncorroded		Corroded	
		$\Delta\sigma_i$	$\Delta\sigma_R$	$\Delta\sigma_i$	$\Delta\sigma_R$
		[Mpa]	[Mpa]	[Mpa]	[Mpa]
Kombi (1)	56.10	6.05	8.16	6.60	8.91
Sedan(1)	73.04	7.87	10.63	8.60	11.60
Stationwagon (1)	73.04	7.87	10.63	8.60	11.60
SUV/Minivan (1)	94.6	10.20	13.76	11.13	15.03
Pickup/Van (1)	130	14.01	18.91	15.30	20.65
Traktor/Smaller trucks (1)	281.6	30.35	40.97	33.14	44.74
Lorry 1 FLM4 (1)	453.20	48.84	65.94	53.34	72.01
Lorry 2 FLM4 (1)	707.85	76.29	102.99	83.31	112.47
Lorry 3 FLM4 (1)	856035	92.29	124.60	100.79	136.06
Lorry 4 FLM4 (1)	657.25	70.84	95.63	77.35	104.43
Lorry 5 FLM4 (1)	694.65	74.87	101.07	81.75	110.37
Kombi (2)	56.10	6.05	8.16	6.60	8.91
Sedan(2)	73.04	7.87	10.63	8.60	11.60
Stationwagon (2)	73.04	7.87	10.63	8.60	11.60
SUV/Minivan (2)	94.6	10.20	13.76	11.13	15.03
Pickup/Van (2)	130	14.01	18.91	15.30	20.65
Traktor/Smaller trucks (2)	281.6	30.35	40.97	33.14	44.74
Lorry 1 FLM4 (2)	453.20	48.84	65.94	53.34	72.01
Lorry 2 FLM4 (2)	707.85	76.29	102.99	83.31	112.47
Lorry 3 FLM4 (2)	856035	92.29	124.60	100.79	136.06
Lorry 4 FLM4 (2)	657.25	70.84	95.63	77.35	104.43
Lorry 5 FLM4 (2)	694.65	74.87	101.07	81.75	110.37

6.5 Nominal stress results based on alternative fatigue vehicle load

6.5.1 Fatigue strength for structural steel components (Uncorroded Steel)

The DIP 95 is a rolled section with an applied bending, and in this instance, the bottom flange will generate tension related to fatigue failure. According to Eurocode, as mentioned in section 3.2.3 and illustrated in figure 3.3, if the fatigue stresses are in tension parallel to the bottom flange, then detail category 160 with constructional detail number 2 is chosen.

An S-N curve that provides information about the fatigue life capacity is shown in below figure.

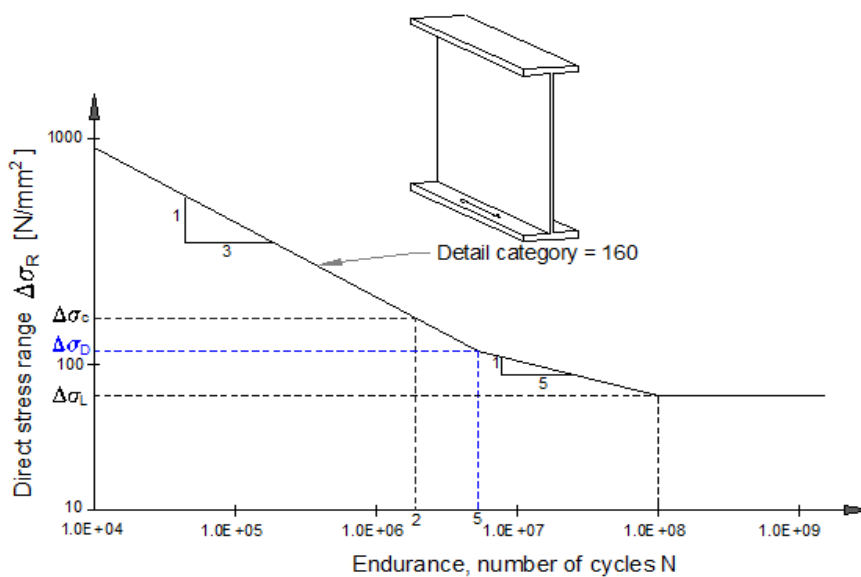


Figure 6.13: Design S-N curve for detail category 160

6.5.2 Fatigue strength for structural steel components

Depending on the number of cycles that would result in fatigue failure for all cases, we can now evaluate what fraction of the overall damage was produced by the various stress ranges over time. This way, we can determine how much of the total damage occurred.

Table 6.8: Results of damage calculations using the Eurocode-based damage accumulation method and the proposed fatigue damage model.

Fatigue Load Model	Fatigue damage calculation	
	Eurocode damage accumulation	Proposed method Aeran et al. [5]
FLM 4	0.003512	0.006947
Scenario 1	0.001468	0.002910
Scenario 2	0.003141	0.006227
Scenario 3	0.005504	0.010911

6.6 Fatigue damage of corroded steel

A proposed formula for calculating fatigue strength of the corroded detail is briefly described in chapter 4. To determine number of cycles until fatigue failure of corroding structural features, equation 12 and 13 can be solved with regard to N_R .

If $\Delta\sigma_{cor} \geq \Delta\sigma_{D,cor}$

$$N_R = \left[\frac{\Delta\sigma_{cor}}{\Delta\sigma_D \cdot N_{f,LCF}^c \cdot N_{f,CAFL}^{\frac{1}{m}}} \right]^{\frac{1}{c-\frac{1}{m}}} \quad (17)$$

If $\Delta\sigma_{cor} \leq \Delta\sigma_{D,cor}$

$$N_R = N_{f,CAFL} \left[\frac{\Delta\sigma_{cor}}{\Delta\sigma_{D,cor}} \right]^{\frac{1}{c}} \quad (18)$$

The values of $N_{f,LCF}$ and N_{CAFL} is given in Tabel 4.1. The stress range at the intersections of two fatigue curve slopes of corrosive-environment-exposed features, which corresponds to $N_{f,CAFL}$:

$$\Delta\sigma_{D,cor} = 0.497 \cdot \Delta\sigma_D \quad (19)$$

The stress range corresponding to $N_{f,VAFL}$ cycles of corrosive-environment-exposed details is [7]:

$$\Delta\sigma_{L,cor} = 0.356 \cdot \Delta\sigma_L \quad (20)$$

6.6.1 Using the proposed method for calculating fatigue life

The predicted fatigue life considering corrosion of 4 mm observed after 81 years can be found as follows:

$$Fatiguelife = \left[\frac{(1 - 81.D_i)}{D_{i,cor}} + 81 \right] \quad (21)$$

where,

D_i is the damage per year for uncorroded elements.

$D_{i,cor}$ is total damage accumulated in the corroded element.

6.6.2 Fatigue strength for structural steel components

Adasooriya et al. [7] experimented with assessing the impact of corrosion while also considering the effect of progressive thickness reduction. The research showed that steel components exposed to hostile environments experienced a significant decrease in fatigue performance. The findings demonstrated this phenomenon, which a modification can characterize the design fatigue strength curves of connection categories and detail classes.

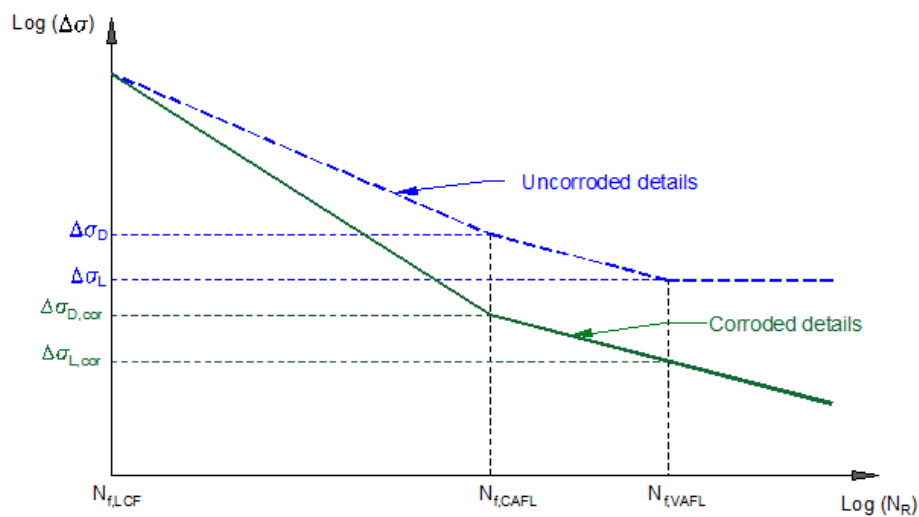


Figure 6.14: Schematic representation of fatigue strength curve of uncorroded and corroded details categories

In detail, formula 22 predicts the remaining fatigue life based on the accumulated damage.

$$Faiquelife = \frac{1}{D_i} \quad (22)$$

The results of the damage calculations using the Eurocode-based damage accumulation method and the proposed fatigue damage model are shown in the table below. After considering the newly suggested corrosion parameter, this computation was performed and subjecting the material to environmentally assisted cracking.

Table 6.9: Results of damage calculations using the Eurocode-based damage accumulation method and the proposed fatigue damage model.

Fatigue Load Model	Fatigue damage calculation	
	Eurocode damage accumulation	Proposed method Aeran et al. [5]
FLM 4	0.052596	0.103981
Scenario 1	0.013530	0.027979
Scenario 2	0.026151	0.052941
Scenario 3	0.043977	0.088196

7 Case studies

This chapter is divided into four different case studies. Each case study is designed to entail the proposed models demonstrated in chapter 4. The application of these models is tested to predict the fatigue life of the Storåna I bridge using FLM4 and alternative traffic load. The case studies are categorized in a manner that aligns each proposed model with either FLM4 or alternative traffic load. This is done to investigate the results produced by the individual models when considering various traffic loads.

7.1 Case study-1

In case study-1, the expected lifetime for FLM 4 is determined using the Eurocode, calculated with Miner's rule, ignoring corrosion wastage. According to the Eurocode, each truck in the model is presumed to cross the bridge without other vehicles. On the contrary, Adasooriya et al. [7] method considers corrosion. Table 7.1 shows the results obtained from both approaches. The outcomes from the application of both models show a significant difference in the expected lifetime of the bridge. The proposed model's difference from Miner's rule is 66.9%.

Table 7.1: Fatigue life results for case study-1

Fatigue Load Model	Fatigue life results (in years)	
	Conventional Uncorroded	method Corroded Adasooriya et al. method
FLM 4	284	94

7.2 Case study-2

Case study-2 has similarities with case study-1 in terms of used models (approaches). The expected lifetime for alternative traffic model is determined using the Eurocode and calculated with Miner's rule by leaving out corrosion wastage. On the other hand, Adasooriya et al. [7] method considers corrosion.

Nonetheless, case study-2 varies from case study-1 when contemplating traffic loads. As shown in Table 6.6, the alternative traffic load model considers different vehicles moving in one and

two lanes. An alternative traffic load model was presented to compare FLM 4, proposed by the Eurocode, with a traffic load model that describes the entire traffic spectrum, not just heavy vehicles. Hence, an alternative traffic load model was presented. The principal objective was to determine how adding more vehicle classes would affect the cumulative damage.

Table 7.2: Fatigue life results for case study-2

Alternative Load Model	Fatigue life results (in years)	
	Conventional method for uncorroded	Adasooriya et al. [7] method for corroded
Scenario 1	681	146
Scenario 2	318	109
Scenario 3	181	93

Table 7.2 shows the results obtained from both approaches. The outcomes from the application of both models show a significant difference in the expected lifetime of the bridge. The proposed model's difference from Miner's rule is 79.00 % in scenario 1, 65.72 % in scenario 2, and 48.62 % in scenario 3.

The examination of individual scenarios in Miner's rule stipulates that the estimated fatigue life decreases immensely, moving downwards from scenario 1 to scenario 3, i.e., $681 > 318 > 181$. The same trend holds while investigating individual scenarios regarding Adasooriya's rule; i.e., the estimated fatigue life decreases tremendously, moving downwards from scenario 1 to scenario 3, i.e., $146 > 109 > 93$.

Even though the estimated fatigue lives from the two approaches demonstrate that a deviation exists, both approaches have highlighted that an increasing traffic load results in a lower fatigue life. Scenario 3 is the most vulnerable to fatigue failure.

7.3 Case study-3

Case study-3 resembles case study-1 since Miner's rule is applied to both cases to estimate the fatigue life of uncorroded steel bridges. In addition, much like in case study-1, the expected lifetime for FLM 4 is determined by ignoring corrosion wastage in case study-3 regarding the conventional uncorroded method. However, in case study-3, the calculation of uncorroded fatigue life includes a damage index method proposed by Aeran et al. [5]. Calculating the fatigue

life of uncorroded steel bridge combines Miner's rule, illustrated in equation 5, and Aeran et al.'s method demonstrated in equation 14. On the other hand, calculating the fatigue life of corroded steel bridge integrates equation 19, 20, and 14.

Table 7.3 shows the outcomes of applying the mentioned approaches to steel bridges' uncorroded and corroded fatigue lives. The outcomes from the application of both models show a significant difference in the expected lifetime of the bridge. The uncorroded approach's difference from the corroded approach is 40.56 %.

Table 7.3: Fatigue life results for case study-3

Fatigue Load Model	Fatigue life results (in years)	
	Aeran et al. [5]method for uncorroded	Aeran et al. [5]method for corroded
FLM 4	143	85

7.4 Case study-4

Case study-4 is similar with case study-2 only in terms of used traffic loads. The expected lifetime for alternative traffic model is determined using Miner's rule alongside Aeran's method by leaving out corrosion wastage for uncorroded scenarios. On the other hand, calculating the fatigue life for corroded scenarios involves the integration of equation 19, 20, and 14.

As illustrated in Table 6.6, the alternative traffic load model considers different vehicles moving in one and two lanes. An alternative traffic load model was presented to compare FLM 4, proposed by the Eurocode, with a traffic load model that describes the entire traffic spectrum, not just heavy vehicles. Hence, an alternative traffic load model was presented. The principal objective was to determine how adding more vehicle classes would affect the cumulative damage.

Table 7.4: Fatigue life results for case study-4

Fatigue Load Model	Fatigue life results (in years)	
	Aeran et al. [5]method for uncorroded	Aeran et al. [5] method for corroded
Scenario 1	343	108
Scenario 2	160	90
Scenario 3	91	82

Table 7.4 shows the results obtained from both approaches. The outcomes from the application of both approaches show a significant difference in the expected lifetime of the bridge. The approaches' difference for uncorroded vs. corroded is 68.51 % in scenario 1, 43.75 % in scenario 2, and 9.89 % in scenario 3.

The examination of individual scenarios in uncorroded scenarios stipulates that the estimated fatigue life decreases immensely, moving downwards from scenario 1 to scenario 3, i.e., $343 > 160 > 91$. The same trend holds while investigating individual scenarios regarding corroded scenarios; i.e., the estimated fatigue life decreases tremendously, moving downwards from scenario 1 to scenario 3, i.e., $108 > 90 > 82$.

Even though the estimated fatigue lives from the both approaches demonstrate that a deviation exists, both approaches have highlighted that an increasing traffic load results in a lower fatigue life. Scenario 3 is the most vulnerable to fatigue failure. On a more specific note, scenario 3 in case study-4 is by far the only scenario that showed little deviation when comparing uncorroded with corroded scenarios.

8 Discussion and comparison of the case studies

When a metal is present in a corrosive environment and subjected to alternate cyclic stresses, the metal will be prone to corrosion fatigue (CF). Damage caused by corrosion fatigue is usually more significant than the damage caused by fatigue and corrosion separately. CF can occur at any given location without pitting. The stress range and maximum stress level regulate the start and propagation of CF cracks. The commencement of CF cracks may occur in the absence of pits, and the expansion of CF cracks in steel might be due to post-corrosion reaction [61].

Examining Storåna I bridge leads one to acknowledge that the existence of uniform corrosion might lead to corrosion fatigue resulting in cracking. Around 2000 vehicles per year pass over the road bridge, indicating that the bridge is exposed to alternative cyclic stresses. Moreover, the bridge is built in a marine environment. The combination of a corrosive marine environment and alternative cyclic stresses makes Storåna I bridge more vulnerable to corrosion fatigue.

Comparing the results gathered from the different case studies demonstrated in Chapter 7 is mandatory since various approaches were used to predict the fatigue life of the bridge. Furthermore, differentiating between uncorroded and corroded results alongside the various traffic loads applied is essential.

Taking FLM4 and considering solely uncorroded cases, the deviation resulting from two different approaches can be seen in the Table 8.1. The divergence between the conventional method for calculating the uncorroded fatigue life and the Aeran et al. [5] method for estimating the uncorroded fatigue life of the bridge is 49.65%. This difference is colossal since both approaches contemplate uncorroded steel, yet the gap is significant. This might indicate how Aeran's method might be more accurate when estimating the uncorroded fatigue life of the bridge.

Table 8.1: Comparison of approaches for uncorroded cases-FLM 4

Fatigue Load Model	Fatigue life results (in years)	
	Conventional method for uncorroded	Aeran et al. [5] method for uncorroded
FLM 4	284	143

Investigating FLM4 and considering exclusively corroded cases, the deviation resulting from two different approaches can be seen in the Table 8.2. The divergence between the Adasooriya et al. method [7] for calculating the corroded fatigue life and the Aeran et al. method [5] for

estimating the corroded fatigue life of the bridge is 9.57%. This difference is significant, yet not so substantial as 49.65%, i.e., the divergence that occurred when considering FLM4 alongside uncorroded cases only. The Adasooriya et al. [7] and the Aeran et al. [5] methods were used for corroded steel in Table 8.2. The results produced are in such a close range that both approaches are near precise for estimating the corroded fatigue life of the bridge.

Table 8.2: Comparison of approaches for corroded cases-FLM 4

Fatigue Load Model	Fatigue life results (in years)	
	Adasooriya et al. [7] method for corroded	Aeran et al. [5] method for corroded
FLM 4	94	85

The deviation resulting from two different approaches can be seen in Table 8.3 by examining alternative traffic load models and considering only uncorroded cases. The divergence between the conventional method for calculating the uncorroded fatigue life and the Aeran et al. method [5] for estimating the uncorroded fatigue life of the bridge is 49.63% for scenario 1, 49.69% in scenario 2, and 49.72% in scenario 3.

The examination of individual scenarios in the conventional method stipulates that the estimated fatigue life decreases immensely, moving downwards from scenario 1 to scenario 3, i.e., $681 > 318 > 181$. The same trend holds while investigating individual scenarios regarding Aeran et al. method; i.e., the estimated fatigue life decreases tremendously, moving downwards from scenario 1 to scenario 3, i.e., $343 > 160 > 91$. Though the estimated fatigue lives from the two approaches demonstrate that a deviation exists, both approaches have highlighted that an increasing traffic load results in lower fatigue life. Scenario 3 is the most vulnerable to fatigue failure.

Table 8.3: Comparison of approaches for uncorroded cases-Scenarios

Fatigue Load Model	Fatigue life results (in years)	
	Conventional method for uncorroded	Aeran et al. [5] method for uncorroded
Scenario 1	681	343
Scenario 2	318	160
Scenario 3	181	91

Another deviation from two proposed approaches can be seen in the Table 8.4 by investigating alternative traffic load models and considering corroded cases exclusively. The divergence between the Adasooriya et al. method [7] for calculating the corroded fatigue life and the Aeran et al. method [5] for estimating the corroded fatigue life of the bridge is 26.03% in scenario 1, 17.43% in scenario 2, and 11.83% in scenario 3.

The inspection of single scenarios in the Adasooriya et al. method [7] stipulates that the estimated fatigue life decreases vastly, moving downwards from scenario 1 to scenario 3, i.e., $146 > 109 > 93$. The same trend holds while examining individual scenarios regarding the Aeran et al. method [5]; i.e., the estimated fatigue life decreases tremendously, moving downwards from scenario 1 to scenario 3, i.e., $108 > 90 > 82$. Even though the estimated fatigue lives from the two approaches exemplify that a deviation exists, both approaches have highlighted that an increasing traffic load results in lower fatigue life. Scenario 3 is still the most vulnerable to fatigue failure.

Table 8.4: Comparison of approaches for corroded cases-Scenarios

Fatigue Load Model	Fatigue life results (in years)	
	Adasooriya et al. [61] method for corroded	Aeran et al. [5] method for corroded
Scenario 1	146	108
Scenario 2	109	90
Scenario 3	93	82

The comparison of all the case studies spotlights numerous uncertainties associated with fatigue life evaluation methods that may lead to different outcomes. Reductions in fatigue lifetimes emphasize the need for precise S-N curves for aging bridges to implement conservative maintenance procedures. Due to commonly accessible fatigue damage models, the application of simplified relations in computing stress concentration factors, and the variation in material characteristics, uncertainties may exist. Hence, this leads to inconsistent fatigue life assessment.

9 Conclusion and future directions

9.1 Conclusion

This study aimed to evaluate the fatigue life of a specific steel bridge by using a conventional method (Miner's rule) and two other approaches (models) proposed by Adasooriya et al. [7] and Aeran et al. [5] to investigate various actual traffic loads. The evaluation of the outcomes from applying the conventional and two proposed models to fatigue load model 4 and alternative traffic loads was then compared and discussed.

The results from considering FLM4 and uncorroded cases exclusively indicates that the Aeran et al. method [5] for estimating the uncorroded fatigue life of the bridge gave a lower fatigue life than the conventional method (Miner's rule). Further findings when taking FLM4 and accounting for corroded cases only implicate that the results produced are in such a close range that both the Adasooriya et al. [7] and the Aeran et al. [5] approaches are near precise for estimating the corroded fatigue life of the bridge. Even though the results were in close range, the Aeran et al. [5] approach produced a lower fatigue life than the Adasooriya et al. [7] method.

Moreover, considering alternative traffic models and uncorroded cases alone indicates that the estimated fatigue life decreases immensely, going from scenario 1 to scenario 3 when using both the conventional and the Aeran et al. [5] methods. However, the Aeran et al. [5] method gave significantly lower fatigue life when compared to the conventional method. Furthermore, contemplating alternative traffic models and corroded cases only indicates that the estimated fatigue life decreases tremendously, going from scenario 1 to scenario 3 when using both the Adasooriya et al. [7] and the Aeran et al. [5] methods. Nonetheless, the Aeran et al. [5] method gave a lower fatigue life when compared to the Adasooriya et al. [7] method.

Examining all case studies highlights the inherent uncertainties connected with fatigue life evaluation approaches, which can lead to varying results. Reduced fatigue lives highlight the need for exact S-N curves for aging bridges to perform conservative maintenance operations. The Aeran et al. [5] method produced the lowest fatigue life in all case studies compared to the conventional and Adasooriya et al. [7] methods. Furthermore, a heavier traffic load contributed to a reduced fatigue life in all models.

9.2 Future directions

Consideration could be given to a comprehensive examination of the Storåna I bridge's current condition to recommend life-extension strategies and bridge maintenance. In addition, measurements of the actual traffic load can be undertaken to provide more accurate bridge response ranges. The frameworks discussed in this thesis could also be applied to a case study in which corrosion deterioration is monitored and compared to estimate fatigue life.

References

- [1] Nada Al-Eidan. What are the most dangerous types of corrosion and does the dangerous vary depending on the type of metal?, 2015. Last accessed 21 May 2022.
- [2] Gibson stainless & specialty INC. Corrosion types and prevention, 2017. Last accessed 24 April 2022.
- [3] R Winston Revie. *Corrosion and corrosion control: an introduction to corrosion science and engineering*. John Wiley & Sons, 2008.
- [4] Mohammad Al-Emrani and Mustafa Aygül. Fatigue design of steel and composite bridges. *Göteborg: Chalmers Reproservice*, 2014.
- [5] Ashish Aeran. Life extension of offshore structures: A conceptual framework and fatigue damage models. 2019.
- [6] Julie Sofie Stave Sandviknes. Environment-assisted fatigue of steel bridges: A conceptual framework for structural integrity/life assessment. Master's thesis, uis, 2021.
- [7] Niroosha D Adasooriya. Structural integrity of steel bridges: Environment-assisted cracking. 2020.
- [8] Erica Siviero and Roberto Pavan. Assessment of existing steel bridges: codes and standard. In *IOP Conference Series: Materials Science and Engineering*, volume 419, page 012006. IOP Publishing, 2018.
- [9] T Siwowski. Fatigue assessment of existing riveted truss bridges: case study. *Bulletin of the Polish Academy of Sciences. Technical Sciences*, 63(1):125–133, 2015.
- [10] D WILLIAM, RETHWISCH CALLISTER, and G DAVID. *MATERIALS SCIENCE AND ENGINEERING: An Introduction, 9e Wiley E-text Student Package*. JOHN WILEY & Sons, 2014.
- [11] P Oehme. Damage analysis of steel structures. In *IABSE Proceedings*, pages 139–189, 1989.
- [12] XW Ye, YH Su, and JP Han. A state-of-the-art review on fatigue life assessment of steel bridges. *Mathematical Problems in Engineering*, 2014, 2014.
- [13] John Yeates Mann. *Bibliography on the Fatigue of Materials, Components and Structures: Volume 4*, volume 4. Elsevier, 2013.
- [14] Walter Schütz. A history of fatigue. *Engineering fracture mechanics*, 54(2):263–300, 1996.

- [15] Weicheng Cui. A state-of-the-art review on fatigue life prediction methods for metal structures. *Journal of marine science and technology*, 7(1):43–56, 2002.
- [16] Ralph I Stephens, Ali Fatemi, Robert R Stephens, and Henry O Fuchs. Metal fatigue in engineering. John Wiley and Sons. Inc., New York, 2001.
- [17] Committee on Fatigue, Fracture Reliability of the Committee on Structural Safety, and American Society of Civil Engineers Reliability of the Structural Division. Fatigue reliability. *Journal of the Structural Division*, 108(1):3–23, 25–46, 47–69, and 71–88, 1982.
- [18] Richard Palmer Reed, JH Smith, and BW Christ. The economic effects of fracture in the united states. *National Bureau of Standards Special Publication*, (647-1):1–7, 1983.
- [19] Tom Lassen and Naman Recho. *Fatigue Life Analyses of Welded Structures*. ISTE Ltd, 2006.
- [20] Norman E. Dowling. *Mechanical Behavior of Materials, Engineering Methods for Deformation, Fracture, and Fatigue*,. International Edition. Pearson Education, 2012.
- [21] Arthur Peter Boresi, Richard Joseph Schmidt, Omar M Sidebottom, et al. *Advanced mechanics of materials*, volume 6. Wiley New York, 1985.
- [22] Arthur P. Boresi and Richard J. Schmidt. *Advanced mechanics of materials*. John Wiley & Sons, INC, 2003.
- [23] Fabien Briffod, Takayuki Shiraiwa, and Manabu Enoki. Fatigue crack initiation simulation in pure iron polycrystalline aggregate. *Materials Transactions*, 57(10):1741–1746, 2016.
- [24] Saurindranath Majumdar and JoDean Morrow. *Correlation between fatigue crack propagation and low cycle fatigue properties*. ASTM International, 1974.
- [25] Paupler PGE Dieter. Mechanical metallurgy. m c graw-hill book co., new york 1986. xxiii+ 751 p., dm 138.50. Technical report, ISBN 0–07–016893–8. Crystal Research and Technology, 1988.
- [26] N Norsok. 004, design of steel structures. *Standards Norway, Rev, 2*, 2004.
- [27] Maria M Szerszen and Andrzej S Nowak. Fatigue evaluation of steel and concrete bridges. *Transportation research record*, 1696(1):73–80, 2000.
- [28] BS EN. 1–9: 2005—eurocode 3: Design of steel structures—part 1–9: Fatigue, 2008. *European Committee for Standardization*, 1993.

- [29] Francesco M Russo, Dennis R Mertz, Karl H Frank, Kenneth E Wilson, et al. Design and evaluation of steel bridges for fatigue and fracture—reference manual. Technical report, National Highway Institute (US), 2016.
- [30] ND Adasooriya, D Pavlou, and T Hemmingsen. Fatigue strength degradation of corroded structural details: A formula for s-n curve. *Fatigue & Fracture of Engineering Materials & Structures*, 43(4):721–733, 2020.
- [31] W Zhang and H Yuan. Corrosion fatigue effects on life estimation of deteriorated bridges under vehicle impacts. *Engineering Structures*, 71:128–136, 2014.
- [32] A Almar Næss, H Andersson, T Moan, S Berge, et al. Fatigue handbook. *Tapir, Trondheim*, 1985.
- [33] Milton A Miner. Cumulative damage in fatigue. 1945.
- [34] CG Schilling. Fatigue of welded steel bridge members under variable-amplitude loadings. *NCHRP report*, (188), 1978.
- [35] Subra Suresh. *Fatigue of materials*. Cambridge university press, 1998.
- [36] Gérard Mesmacque, S Garcia, Abdelwaheb Amrouche, and C Rubio-Gonzalez. Sequential law in multiaxial fatigue, a new damage indicator. *International Journal of Fatigue*, 27(4):461–467, 2005.
- [37] Z Hashin and A Rotem. A cumulative damage theory of fatigue failure. *Materials Science and Engineering*, 34(2):147–160, 1978.
- [38] SS Manson and GR Halford. Practical implementation of the double linear damage rule and damage curve approach for treating cumulative fatigue damage. *International journal of fracture*, 17(2):169–192, 1981.
- [39] SS Manson and Gary R Halford. Re-examination of cumulative fatigue damage analysis—an engineering perspective. *Engineering Fracture Mechanics*, 25(5-6):539–571, 1986.
- [40] JH Bulloch. The influence of mean stress or r-ratio on the fatigue crack threshold characteristics of steels—a review. *International journal of pressure vessels and piping*, 47(3):263–292, 1991.
- [41] NE Dowling, CA Calhoun, and A Arcari. Mean stress effects in stress-life fatigue and the walker equation. *Fatigue & Fracture of Engineering Materials & Structures*, 32(3):163–179, 2009.

- [42] David P Kihl and Shahram Sarkani. Mean stress effects in fatigue of welded steel joints. *Probabilistic engineering mechanics*, 14(1-2):97–104, 1999.
- [43] Shyh-Jen Wang and Marvin W Dixon. A new criterion for positive mean stress fatigue design. 1997.
- [44] Ashish Aeran, SC Siriwardane, Ove Mikkelsen, and Ivar Langen. An accurate fatigue damage model for welded joints subjected to variable amplitude loading. In *IOP Conference Series: Materials Science and Engineering*, volume 276, page 012038. IOP Publishing, 2017.
- [45] Lisa Lindquist. *Corrosion of steel bridge girder anchor bolts*. PhD thesis, Georgia Institute of Technology, 2008.
- [46] Robert Kogler et al. Steel bridge design handbook: Corrosion protection of steel bridges. Technical report, United States. Federal Highway Administration. Office of Bridges and Structures, 2015.
- [47] James Howard Bridge. *The Inside History of the Carnegie Steel Company: A Romance of Millions*. University of Pittsburgh Pre, 1992.
- [48] Kenneth R Trethewey and John Chamberlain. Corrosion for science and engineering. 1995.
- [49] Joseph R Davis. *Corrosion: Understanding the basics*. Asm International, 2000.
- [50] Kenneth A Chandler and Derek A Bayliss. Corrosion protection of steel structures. 1985.
- [51] K Trethewey J Chamberlain. *Corrosion for science and Engineering*, chapter 7, 168. Longman Group Limited, London, 2 edition, 1995.
- [52] Chintan Hitesh Patel, Mark D Bowman, et al. Pack rust identification and mitigation strategies for steel bridges. Technical report, Purdue University. Joint Transportation Research Program, 2018.
- [53] JM Kulicki, Z Prucz, DF Sorgenfrei, DR Mertz, and WT Young. *Guidelines for evaluating corrosion effects in existing steel bridges*. Number 333. 1990.
- [54] K Kreislova and H Geiplova. Evaluation of corrosion protection of steel bridges. *Procedia Engineering*, 40:229–234, 2012.
- [55] Mohammadreza Tavakkolizadeh, Hamid Saadatmanesh, et al. Galvanic corrosion of carbon and steel in aggressive environments. *Journal of Composites for construction*, 5(3):200–210, 2001.
- [56] Olguín C Coca and Francisco Javier. Corrosion fatigue of road bridges: a review. 2011.

- [57] R Rahgozar. Remaining capacity assessment of corrosion damaged beams using minimum curves. *Journal of Constructional Steel Research*, 65(2):299–307, 2009.
- [58] Philip A Schweitzer. Fundamentals of corrosion: mechanisms, causes, and preventative methods. 2009.
- [59] Neil G Thompson, Mark Yunovich, and Daniel Dunmire. Cost of corrosion and corrosion maintenance strategies. *Corrosion Reviews*, 25(3-4):247–262, 2007.
- [60] World bank. Trading economics, 2022. Last accessed 24 July 2022.
- [61] ND Adasooriya, Tor Hemmingsen, and Dimitrios Pavlou. S-n curve for riveted details in corrosive environment and its application to a bridge. *Fatigue & Fracture of Engineering Materials & Structures*, 43(6):1199–1213, 2020.
- [62] Ronald N Clark, Robert Burrows, Rajesh Patel, Stacy Moore, Keith R Hallam, and Peter EJ Flewitt. Nanometre to micrometre length-scale techniques for characterising environmentally-assisted cracking: An appraisal. *Heliyon*, 6(3):e03448, 2020.
- [63] Alfred R Mangus. A fresh look at orthotropic technology. *Public roads*, 68(5), 2005.
- [64] Christopher Lerosé. The collapse of the silver bridge. *West Virginia Historical Society Quarterly*, 15(4):1, 2001.
- [65] Tianliang Zhao, Zhiyong Liu, Cuiwei Du, Chunduo Dai, Xiaogang Li, and Bowei Zhang. Corrosion fatigue crack initiation and initial propagation mechanism of e690 steel in simulated seawater. *Materials science and engineering: A*, 708:181–192, 2017.
- [66] Robert Baboian. *Corrosion tests and standards: application and interpretation*, volume 20. ASTM international, 2005.
- [67] ND Adasooriya, Tor Hemmingsen, and Dimitrios Pavlou. Fatigue strength degradation of metals in corrosive environments. In *IOP Conference Series: Materials Science and Engineering*, volume 276, page 012039. IOP Publishing, 2017.
- [68] Edwin Henry Gaylord, Charles N Gaylord, and James E Stallmeyer. *Design of steel structures*. 1992.
- [69] Mohamed Soliman, Dan M Frangopol, and Kihyon Kown. Fatigue assessment and service life prediction of existing steel bridges by integrating shm into a probabilistic bilinear s-n approach. *Journal of Structural Engineering*, 139(10):1728–1740, 2013.
- [70] Krzysztof Śledziwski. Fatigue assessment of bridge structures according to eurocodes. *Czasopismo Inżynierii Lądowej, Środowiska i Architektury*, 2017.

- [71] NS-EN 1991-2:2003+NA:2010. *Eurocode 1: Actions on structures part 2: Traffic loads on bridges*.
- [72] E Alexandra Micu, Abdollah Malekjafarian, Eugene J OBrien, Michael Quilligan, Ross McKinstry, Ewan Angus, Myra Lydon, and F Necati Catbas. Evaluation of the extreme traffic load effects on the forth road bridge using image analysis of traffic data. *Advances in Engineering Software*, 137:102711, 2019.
- [73] Lu Deng, Wangchen Yan, and Lei Nie. A simple corrosion fatigue design method for bridges considering the coupled corrosion-overloading effect. *Engineering Structures*, 178:309–317, 2019.
- [74] Wei Wang, Lu Deng, and Xudong Shao. Number of stress cycles for fatigue design of simply-supported steel i-girder bridges considering the dynamic effect of vehicle loading. *Engineering Structures*, 110:70–78, 2016.
- [75] Jaap Schijve. Fatigue of structures and materials in the 20th century and the state of the art. *International Journal of fatigue*, 25(8):679–702, 2003.
- [76] Turan Dirlik. *Application of computers in fatigue analysis*. PhD thesis, University of Warwick, 1985.
- [77] Paul H Wirsching, Thomas L Paez, and Keith Ortiz. *Random vibrations: theory and practice*. Courier Corporation, 2006.
- [78] Alain Nussbaumer, Luis Borges, and Laurence Davaine. *Fatigue design of steel and composite structures: Eurocode 3: Design of steel structures, part 1-9 fatigue; Eurocode 4: Design of composite steel and concrete structures*. John Wiley & Sons, 2012.
- [79] Dewesoft. Fatigue analysis, damage calculation, rainflow counting., 2022. Last accessed 29 July 2022.
- [80] Martin Macho, Pavel Ryjáček, and Jose Matos. Fatigue life analysis of steel riveted rail bridges affected by corrosion. *Structural Engineering International*, 29(4):551–562, 2019.
- [81] Gunnstein T Frøseth, Anders Rønquist, Daniel Cantero, and Ole Øiseth. Influence line extraction by deconvolution in the frequency domain. *Computers & Structures*, 189:21–30, 2017.
- [82] P Poluraju and N Rao. Pushover analysis of reinforced concrete frame structure using sap 2000. *International Journal of Earth Sciences and Engineering*, 4(6):684–690, 2011.
- [83] Sang-Ho Lee. Implementation framework toward an integrated steel bridge. In *Computational Mechanics: Proceedings of the Sixth World Congress on Computational*

Mechanics in Conjunction with the Second Asian-Pacific Congress on Computational Mechanics, September 5-10, 2004, Beijing, China, page 420. , 2004.

- [84] Xu Zheng, Dong-Hui Yang, Ting-Hua Yi, and Hong-Nan Li. Bridge influence line identification from structural dynamic responses induced by a high-speed vehicle. *Structural Control and Health Monitoring*, 27(7):e2544, 2020.

A Appendix

The figures included in this appendix are obtained from Norwegian Public Roads Administration (Statens vegvesen). Moreover, the calculations performed on Microsoft Excel to produce results can be found within this link ¹ provided in the footnote.

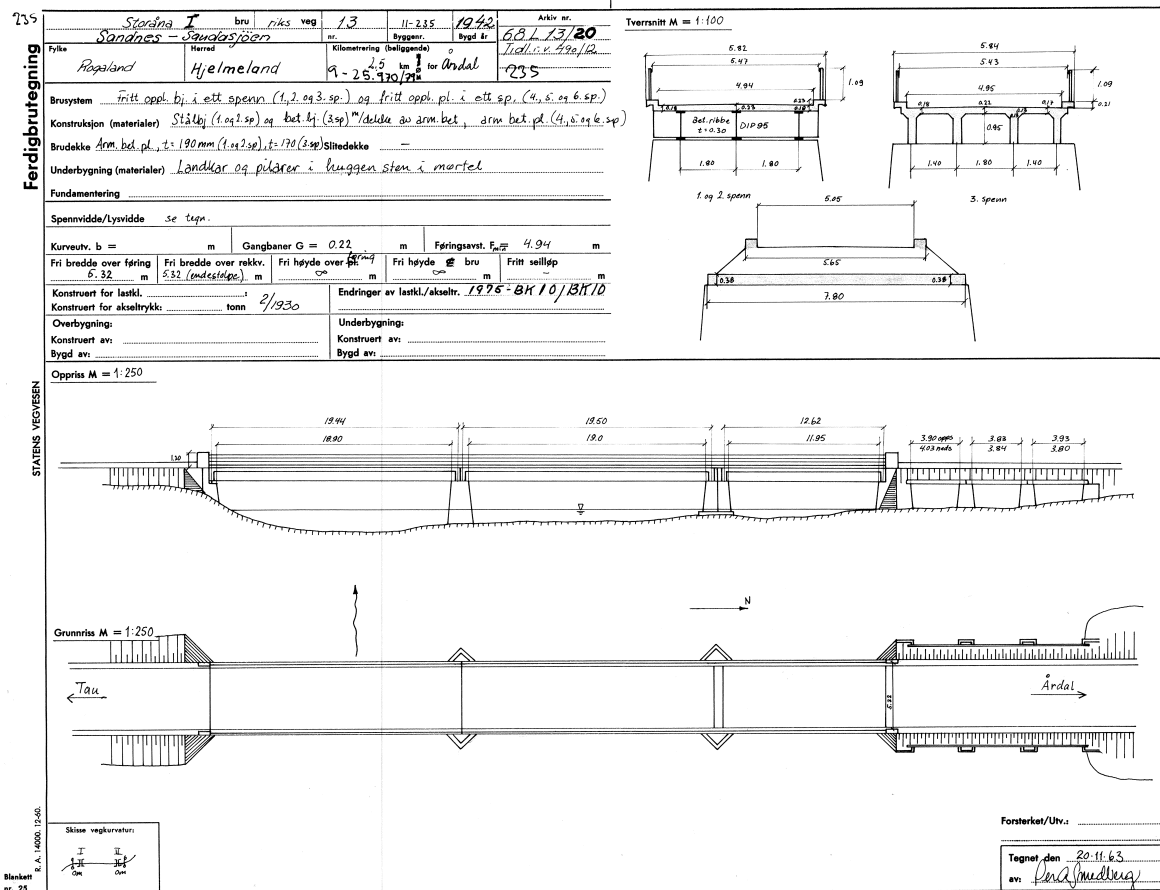
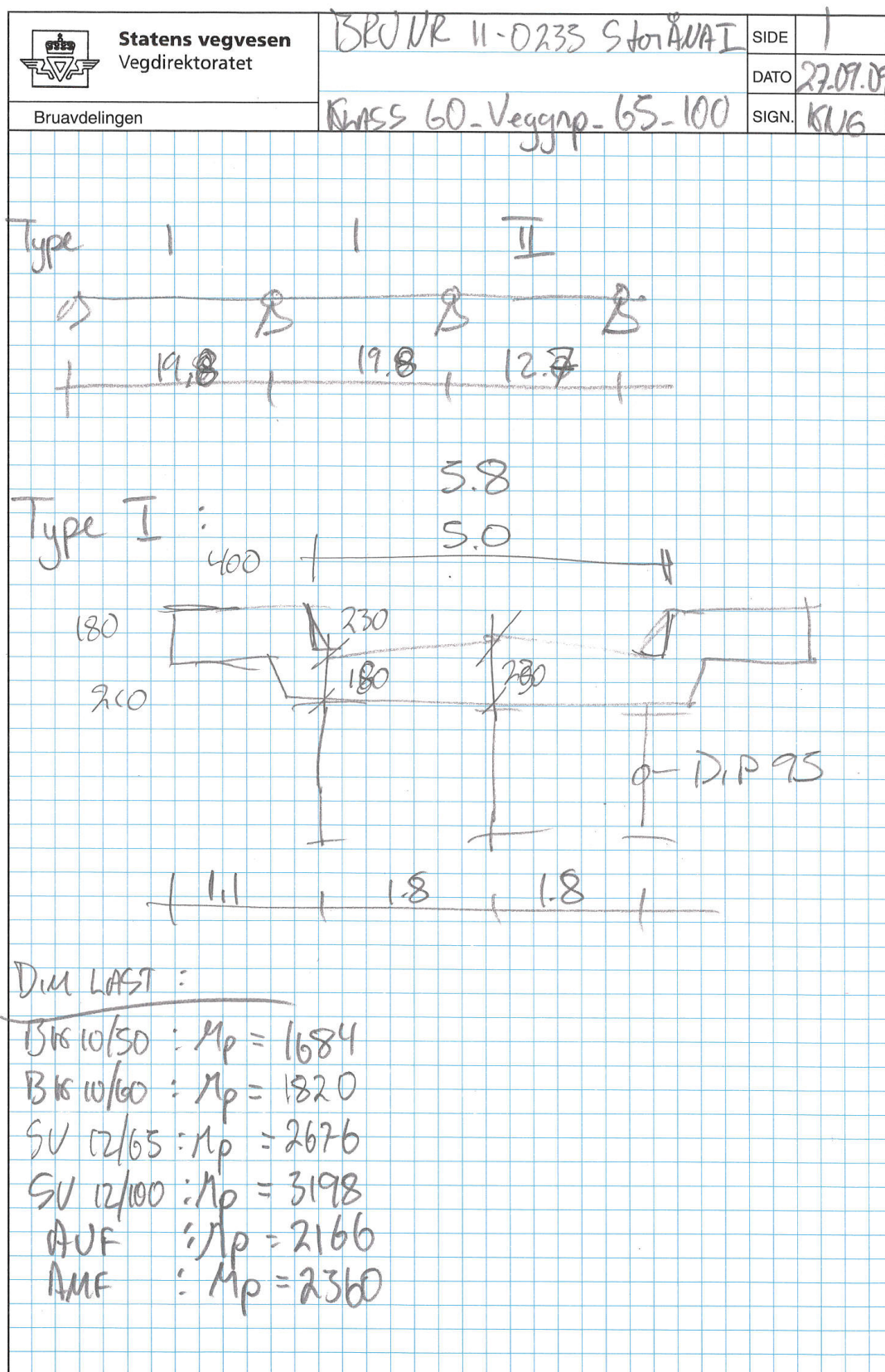


Figure A.1

¹https://drive.google.com/drive/folders/1BhXAPrP7D1GC_q4SYgQOHwoYldRh5zL5?usp=sharing



e.s. Inykk-Oslo

Figure A.2

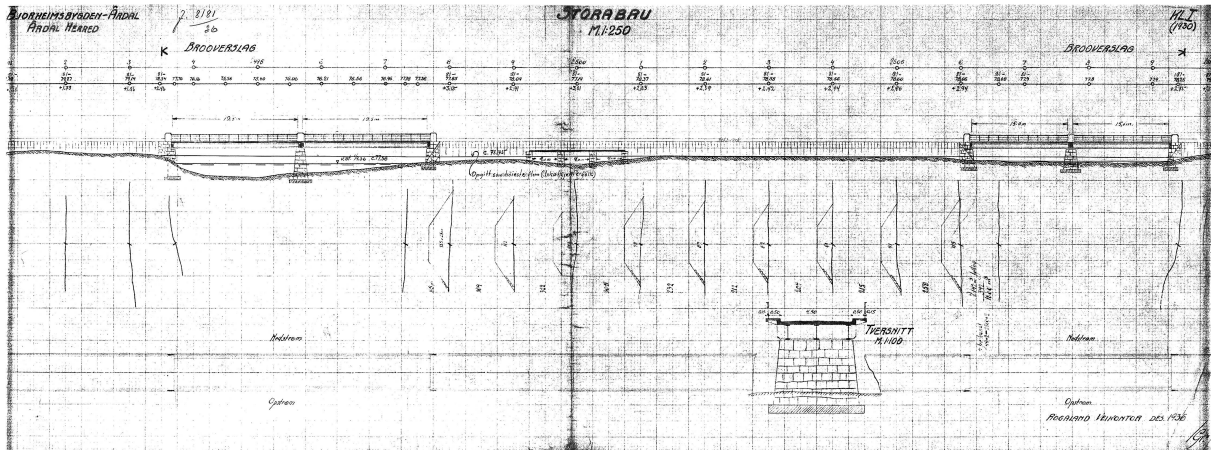


Figure A.3

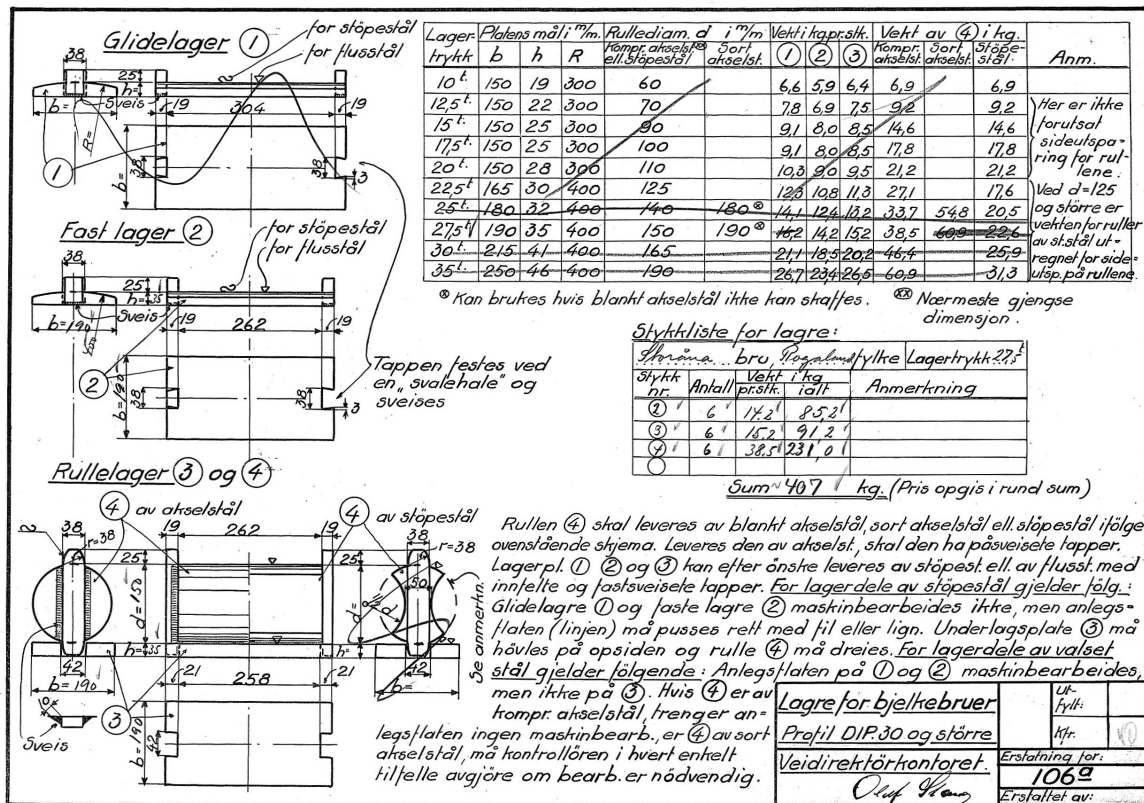


Figure A.4

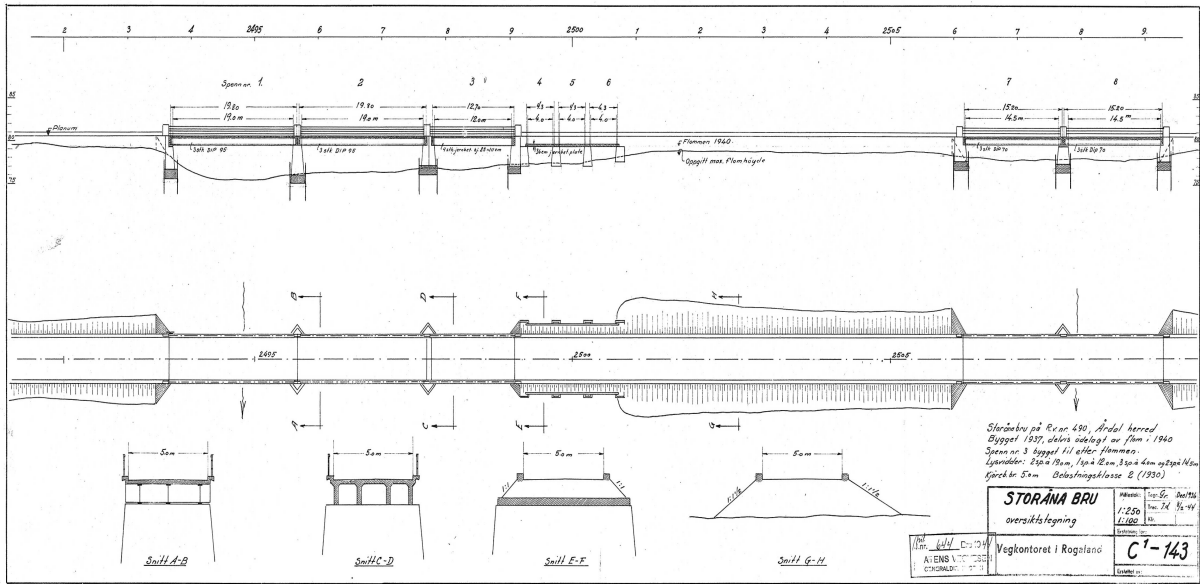


Figure A.5

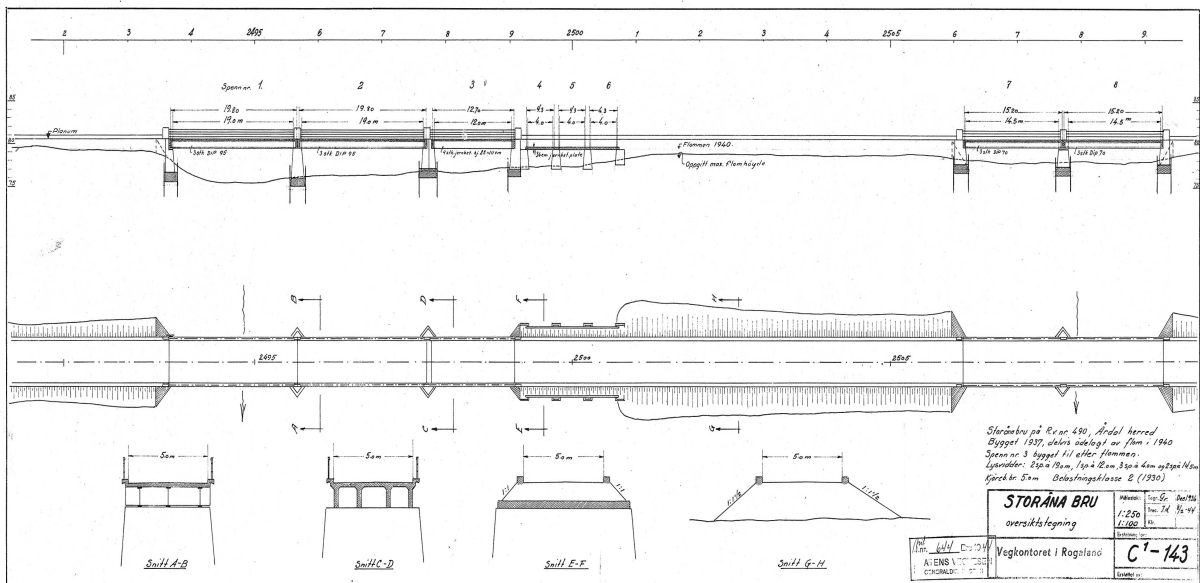


Figure A.6



Figure A.7



Figure A.8



Figure A.9



Figure A.10



Figure A.11



Figure A.12

Byggverk	Vegreferanse	Kategori / type	Lengde / Antall spenn	Start akse	Slutt akse	Bru over
11-0235 Storåna I	P/RV13 S6D1 m7519	Vegbru / Stålbjelkebru	70.0 / 6	1-Mot Tau	7-Mot Årdal	Elv/Innsjø

Inspeksjonsrapport

Byggeværksmerknad
Bygd i 1937, delvis ødelagt av flom i 1940. Bygd opp igjen og utvidet til som i dag i 1942. Bor renses under (varmveisling e.l.) og sprøytet på tørrbetong I spenn 1 og 2 er det benyttet DIP 95, dekke t=19cm. Dekke spenn 3 t=17cm. Dekke spenn 4, 5 og 6 t=38cm. Nytt rekkverk ble satt opp vinter 2012 Bruarkiv vegdir.: JA Originaltegning vegdir.: E3

Tiltak

Tiltakstype	Beskrivelse	Årsak	Oppdragsansvarlig	Utførelsesdato	Intervall	Status	Kostnad	Merknad
Vedlikehold	Fjern vegetasjon pilarer			11.07.2021		Planlagt		
Vedlikehold	Renske betong og armering, samt mørtling. Gjelder hovedbjelke i betong og brudekke.			11.07.2021		Planlagt		
Vedlikehold	Rense og påføre nytt malesystem på hovedbjelker av stål			11.07.2021		Planlagt		

Inspeksjonsplan

Inspeksjonstype	Sist utført	Intervall	Planlagt utført	Tilkomst
Enkel inspeksjon	03.05.2021	1	03.05.2022	Ikke behov
Hovedinspeksjon	11.07.2018	5	11.07.2023	Ikke behov
Hovedinspeksjon u/vann	07.12.2018			Annet

Inspeksjonsdata

Utførelsesansvarlig	Utførelsesdato

Inspeksjonsmerknad
Ingen merknad er angitt

11-0235 Storåna I

Side 1 av 11

Rapport hentet ut: 08.03.2022

Figure A.13